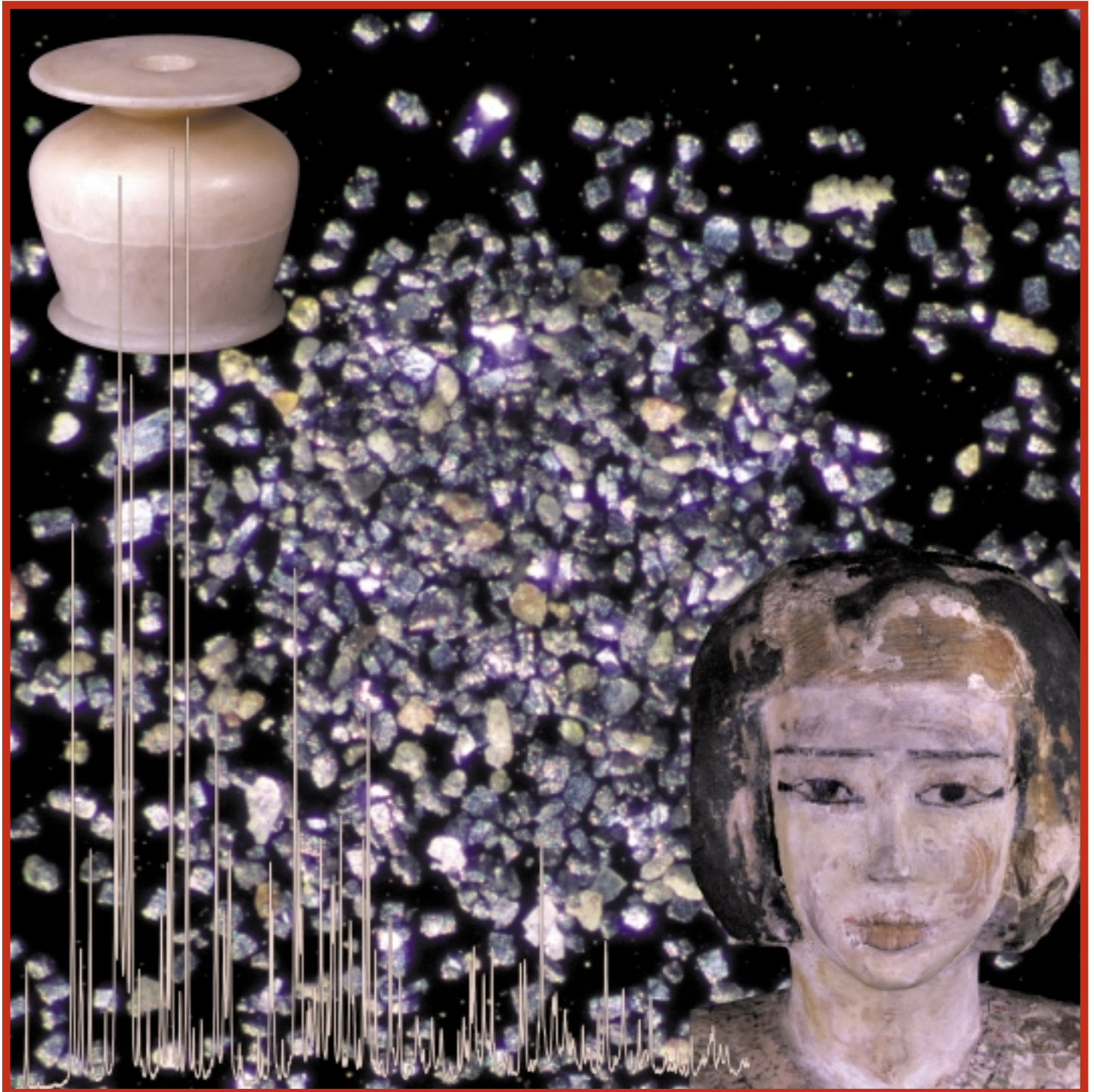


ESRF NEWSLETTER

APRIL 1999

EUROPEAN SYNCHROTRON RADIATION FACILITY

N° 32



New insight into make-up used in Ancient Egypt: the x-ray diffraction pattern measured on BM16 reveals the recipes of the cosmetics made from synthetic and natural lead compounds to beautify and treat the eye. The micrograph of the powder preserved for 3500 years in this alabaster receptacle shows nicely faceted galena crystals (about 50 μm).

ISSN 1011-9310

THE NEWS MAGAZINE OF THE ESRF - ALSO AT <http://www.esrf.fr/info/science/newsletter>

CONTENTS

- NEWSLETTER** Appointment of a New Director General, PAGE 2.
- IN BRIEF** ESRF Users' Meeting, PAGE 3, M. Cooper.
Materials Science at Third Generation Synchrotron Radiation Facilities, PAGE 4, Å Kvick.
Frontiers in SAXS and SANS - 99, PAGE 4, O. Diat.
Workshop on X-ray Magnetic Circular Dichroism, PAGE 5, J. Goedkoop.
BioXAS Workshop, PAGE 6, M. Borowski.
Report from HERCULES 1999, PAGE 6.
Euroconference and NEA Workshop Actinide-XAS-98, PAGE 7, T. Reich.
30th Council Meeting, PAGE 8, K. Witte.
New Science Advisory Committee, PAGE 8.
Latest Beam Time Requests, PAGE 9, R. Mason.
New Measures for the Life Sciences Users, PAGE 9, R. Mason.
- EXPERIMENTS** Cosmetic Recipes and Make-up Manufacturing in Ancient Egypt, PAGE 10, P. Martinetto, E. Dooryhee,
REPORTS M. Anne, J. Talabot, G. Tsoucaris and Ph. Walter.
First Observation of a Magnetic Speckle Pattern by Coherent X-ray Scattering at the Uranium M_{IV} Edge,
PAGE 12, F. Yakhou, A. Létoublon, F. Livet, M. de Boissieu, F. Bley and C. Vettier.
X-ray Resonant Scattering and Orbital Order in V_2O_3 , PAGE 14, L. Paolasini, C. Vettier, F. de Bergevin,
D. Mannix, W. Neubeck, A. Stunault, F. Yakhou, J.M. Honig and P.A. Metcalf.
Determination of the Infinite Frequency Sound Velocity in the Glass Former Ortho-terphenyl, PAGE 16,
G. Monaco, C. Masciovecchio, G. Ruocco and F. Sette.
Radiation Trapping in Resonant Nuclear Scattering of X-rays, PAGE 18, A.I. Chumakov, J. Metge,
A.Q.R. Baron, R. Rüffer, Yu.V. Shvyd'ko, H. Grünsteudel and H.F. Grünsteudel.
Angular Resolved Density of Phonon States, PAGE 19, A.I. Chumakov, R. Rüffer, A.Q.R. Baron, H. Grünsteudel,
H.F. Grünsteudel and V.G. Kohn.
Stroboscopic Diffraction Imaging of High-Frequency Surface Acoustic Waves, PAGE 20, E. Zolotoyabko,
D. Shilo, W. Sauer, E. Pernot and J. Baruchel.
3D Visualization of Snow Samples by Microtomography at Low Temperature, PAGE 22, J.-B. Brzoska,
C. Coléou, B. Lesaffre, S. Borel, O. Brissaud, W. Ludwig, E. Boller and J. Baruchel.
- EVENTS** Users' Meeting.
Young Scientist Award.
Appointment of a new Director General.

Photography by:

*G. Admans, C. Argoud,
E. Boller, B. Denis (Art Photos).*

APPOINTMENT OF A NEW DIRECTOR GENERAL

The ESRF Council has opened the selection for the appointment of a new Director General of the ESRF to come into office in January 2001. As a first step the eight delegations to the ESRF Council are invited to nominate candidates. People interested in contributing to this phase, for example by suggesting candidates, may contact one of the Heads of Delegations listed hereunder, by **30 April 1999**:

FRANCE: J.P. Pouget (CNRS)
e-mail: nathalie.godet@cnrs-dir.fr

GERMANY: A. Freytag (BMBF)
e-mail:
arno.freytag@bmbf.bund400.de

ITALY: C.M. Bertoni
(Università di Modena)
e-mail: bertoni@unimo.it

UNITED KINGDOM: S. Ward (EPSRC)
e-mail: stuart.ward@epsr.ac.uk

BENESYNC (BELGIUM, THE NETHERLANDS):
J. Traest (FWO)
e-mail: jose.traest@nfwo.be

SPAIN: J.M. Calleja
(Universidad Autonoma de Madrid)
e-mail: jose.calleja@uam.es

SWITZERLAND: J.P. Ruder (BBW)
e-mail:
jean-pierre.ruder@bbw.admin.ch

NORDSYNC
(DENMARK, FINLAND, NORWAY, SWEDEN):
R. Feidenhans'l
(Risø National Laboratory)
e-mail: fys-rofe@risoe.dk



ESRF USERS' MEETING

11 February 1999

The history books show that this was the ninth meeting of ESRF users, although the first few took place at times when there was little to use, but lots to talk about. Now there are so many results that a one day meeting can do little more than highlight a few areas and offer a market place for the vast majority to display their results on posters for all to see.

This year 474 people registered for the meeting which is a record, or near record. They were doubtless drawn to Grenoble by the associated workshop program which is described hereafter. Suffice it to say that the three workshops were all over-subscribed and the auditoria were full to their legal capacity. Of course we hoped that many would also be drawn by the opportunity to refine their beam time applications with just a fortnight to go before the submission deadline. We also suspected that several would be tempted to take to the hills at the earliest opportunity. Whatever the reason they all came and Mother Nature took a hand in deciding to confine us all to Grenoble by dumping an unreasonably large amount of snow on top of the meeting!

The meeting began with reports from the ESRF Directors covering the operation of the machine (good and getting better), the completion of beamlines (almost done), the competition for beam time (higher ever higher) and some examples of the scientific activity (where is that Nobel Prize?).

The first of the highlight talks was given by J. Laissue (Berne) on the micro-beam-therapy pre-clinical studies on ID17. Both W. Thomlinson, who introduced the talk and J. Laissue paid tribute to P. Spanne whose death in the Swissair crash was a tragic loss to the Medical Beamline. The very encouraging results for the «sparing» of benign tissue obtained with the use of a microslit/multislit collimator were described.

After coffee the focus moved to the work of the Scientific Advisory Committee (SAC) which advises the ESRF Council. R. Fourme, the SAC Chairman, discussed its work and described its guiding role in the facility's development. He ended with

some thoughtful points about the iniquities of short-term contracts for young scientists on whose unstinting efforts institutions like ESRF rely. We reported on the users' perception of ESRF as revealed by questionnaires, floor tours etc. and were happy to confirm that there are few complaints and plenty of compliments. W. Schulke (Dortmund) then described the selection process for the Young Scientist Award and announced the winner: Peter Cloetens who works on the topography beamline. Peter came to Grenoble in 1994 after graduating in engineering from the Vrije Universiteit Brussels. During experiments on BM5 he observed that objects with negligible absorption can be imaged in a monochromatic beam and over the following three years he explored this phenomenon both experimentally and theoretically and exploited it to study a number of problems in materials science as well as developing, with an Italian team, a wave guide to produce a submicron coherent divergent source and hence the first magnified phase contrast images. Peter received the award (5,000 French Francs - next year 762 Euros?) and gave an excellent account of his work.

The afternoon's highlights came from physics, biology and chemistry. Firstly L. Paolasini (ESRF) described the heroic resonant scattering experiments carried out at ID20 which provide the first direct evidence for orbital ordering in addition to the

more familiar magnetic ordering in $(V_xCr_{1-x})_2O_3$. He made light work of describing this truly complex piece of physics despite a power cut to the overhead projectors! The true extent of his work was revealed by an innocent question about getting «more data». L. Paolasini calmly explained just how much sweat and tears were involved in putting those vital few points on the curve!

E. Garcin (IBS, Grenoble) then described the characterization of metal sites in hydrogenases using anomalous dispersion methods on BM14 and BM2. These materials are the metalloenzymes that are involved in hydrogen biocatalysis: they are «vital» materials. The beautiful experiments she described were able to pinpoint all the metal sites and their ligands.

The final highlight talk was given by a physicist - E. Isaacs (Lucent Technologies New York) talking about chemistry: the covalency of the hydrogen bond in ice, which was first discussed by Pauling. The experiment that at last validated this concept was incoherent Compton scattering, rather than coherent diffraction. The study was carried out at ID15 and E. Isaacs showed how a simple analysis of the broadened Compton profile provided evidence - the first direct evidence - for substantial covalent character to the bond.

The session at Atria continued with a well-attended poster session that amply filled the space and time

*P. Cloetens
receiving the
Young
Scientist
Award from
W. Schulke.*





... ESRF USERS' MEETING

available. Indeed at the end of the afternoon it was difficult to persuade everyone to brave the snow and drift back to the ESRF. Over 300 managed this in time to partake in an excellent dinner. Those of us who had been involved in choosing the food and the wines made every attempt to ensure that all our choices were excellent and indeed they were!

On behalf of the Organizing Committee I would like to thank everyone for their help in making this such a successful meeting. Especial thanks are due to the speakers who clearly had made an effort to tailor their talks to the «SR family» audience and to the ESRF staff who helped to ensure that everything went smoothly. The User

Office staff, who bear the brunt of the organization were devastated by flu in the two previous weeks, nonetheless they worked so hard that you would have never known it. Thank you.

Now what do we do to make next year even better? It will be our 10th so it must be special. What ideas do you have? The date will be Thursday 10 February 2000, by which time you will have recovered from millennium parties and millennium bugs. Suggestions for workshops, prayers for a little less snow and inoculations against flu should start now.

M. Cooper,
on behalf of the ESRF
Users Organization



M. Cooper

MATERIALS SCIENCE AT THIRD GENERATION SYNCHROTRON RADIATION FACILITIES

12 February 1999

A workshop entitled "Materials Science at Third Generation Synchrotron Radiation Facilities" was organized by P. Withers, Univ. of Manchester and Å. Kvick, ESRF, on 12 February after the ESRF Users' Meeting. The Director General Y. Petroff opened the meeting, which featured 13 invited speakers and a poster session. Various aspects of stress and strain measurements were covered by P. J. Webster, A. Pyzalla, W. Jark, O. Castelnau, I. C. Noyan and U. Pietsch. H. Poulsen described a new 3-DXRD microscope implemented at ID11 for materials science characterization. *In situ* studies of nucleation and transformations in polyethylenes and metallic glasses were discussed by S. Rastogi and

A. Yavari. Time-resolved studies of self-propagating high-temperature synthesis and functional materials were presented by M. A. Rodriguez and P. Barnes. B. Salbu showed how radionuclides released by nuclear accidents could be traced by a combination of synchrotron radiation micro-beam techniques and electron microscopy. M. Drakopoulos explained how coherent illumination could be used to study micro-electronics structures. The workshop was concluded by a very active poster session featuring in excess of 30 posters. The workshop was very well received and the attendance was between 120 and 150 participants.

Å. Kvick

FRONTIERS IN SAXS AND SANS - 99

12/13 February 1999

Small-angle scattering is a well-established technique to characterize structures ranging from nanoscopic (1 nm) to microscopic (a few microns) scales. A combination of small-angle x-ray scattering (SAXS) and small-angle neutron scattering (SANS) provides complementary (contrast) structural information in a myriad of systems belonging to hard, soft as well as biological matter. On Friday 12 and Saturday 13 February, a common ESRF-ILL-CEA workshop was held at the ILL organized by T. Zemb (CEA-Saclay), B. Deme (ILL), O. Diat (CEA, Grenoble) and T. Narayanan (ESRF). The purpose of this workshop was to provide a comprehensive overview of the state-of-the-art instruments existing at the ESRF and ILL to the current and prospective users.

The workshop comprised seven oral sessions, one poster session, and visits to the beamlines/instruments. In the first session, the beamline/instrument scientists presented the current status of the respective stations/instruments. The following five sessions were primarily dedicated to discuss the present limits in spatial and time resolutions. These sessions covered many of the recent developments in optics, detectors, and sample environments, and stressed the need for further improvements. The closing session demonstrated the power of small-angle scattering as applied to two different situations involving, one protein solutions and the other solid polymers.

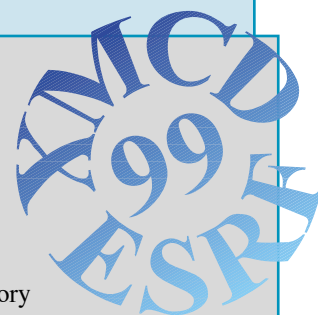
About 120 researchers (including the invited speakers) from France, Germany, UK, Italy, Spain, Netherlands, Sweden, Finland, and Austria participated in this workshop. The workshop further emphasized the usefulness of bringing both the x-ray and neutron communities together for joint endeavors.

T. Zemb



WORKSHOP ON X-RAY MAGNETIC CIRCULAR DICHOISM

12/13 February 1999



XMCD99 turned out to be a very lively gathering, attended by about 100 scientists, a good part of the world's small x-ray magneto-optical community. XMCD stands for X-ray Magnetic Circular Dichroism, the effect in which the x-ray «colour» (~ absorption coefficient) changes under inversion of the handedness of the circular polarization of the x-rays. It has a linearly polarized counterpart and, since the recent work at ESRF, also a «natural», or non-magnetic one. X-ray dichroism occurs also in derived spectroscopies, such as photoemission and x-ray scattering. In all cases it is especially strong at absorption resonances.

X-ray dichroic effects have been studied for the last 12 years, but XMCD99 illustrated that the field is still on the steep part of the learning curve, with an explosion of the use of the fundamental effect in many different directions. The organizers intended to focus the workshop on the so-called XMCD sum rules, a theoretical result that promises the separate measurement of the spin and the orbital parts of the magnetic moment. Since the orbital moment plays a key role in determining the magnetic anisotropy, which in turn defines the magnetic hardness, these rules are in principle extremely useful for magnetic research. However, there have been far more theory papers than experimental papers on

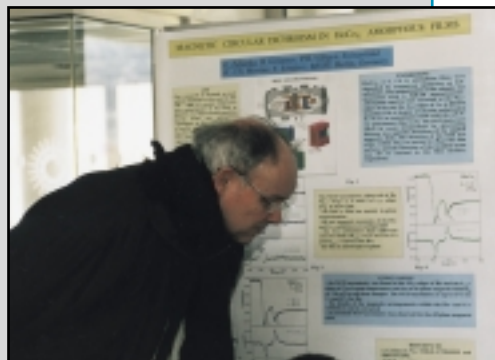
the subject, due to the difficulty of the experiment, which is very difficult without third-generation sources of polarized x-rays.

Indeed, also at XMCD99 new theoretical sum rules were presented, giving an even more precise direct link between linear dichroism and magnetic anisotropy, as well as sum rules for the newly discovered natural dichroism and for magnetic EXAFS. In addition several experiments gave beautiful illustrations of the use of sum rules in «real world» magnets such as $\text{Nd}_2\text{Fe}_{14}\text{B}$, magnetic multilayers and thin films, and Invar systems under high pressure. A new theme that could be picked from these talks is the intimate connection between the orbital moment, anisotropy and tetragonal distortions from octahedral symmetry.

The most fascinating aspect of the workshop was, however, that it showed the proliferation of the use of X-ray Magnetic Dichroism to obtain magnetic contrast. The talks on imaging and scattering showed convincingly how magnetic domain structures and magnetic roughness can be measured at scales of 50-1500 Å, not only in but also below the surfaces of magnetic thin films. The American input in this respect showed the power of these techniques to characterize magneto-electronical devices such as spin valves and the new non-volatile Magnetic Random

Access Memory (MRAM).

Another completely new direction is the use of the bunch structure of ESRF to study the magnetic relaxation of such thin film structures after a synchronous magnetic pulse excites them.



Together, all these developments show that the field is very much alive, and the general feeling was that it will be worthwhile to continue with XD2000, a broader name to do justice to the diversity of subjects. The organizers of the '99 version would not be afraid at all of doing the job again, thanks to the incredibly professional support that they obtained from the ESRF staff, the User Office, and in particular F. Mengoni (Theory Group), who made organizing it a great pleasure.

J. Goedkoop

For the program and abstracts, see <http://www.esrf.fr/conferences/XMCD99/>





BIOXAS WORKSHOP

15/16 February 1999

A workshop on X-ray Absorption Spectroscopy for Biology using a third generation source was held at the ESRF on 15 and 16 February 1999. Speakers and participants from Europe and the United States gave a statement of the current developments in the field. New possibilities, but also problems associated with the investigation of biological samples using X-ray Absorption Spectroscopy

(XAS) using the high flux of 3rd generation synchrotron sources, and the complementary use of different techniques were discussed during the workshop organized by the EXAFS Group (A. Solé, S. Pascarelli, M. Borowski and J. Goulon) and P. Lindley.

The interest of the scientific community is underlined by the November report of the European

Science Foundation (ESF) concerning the needs of the bio-science community with respect to synchrotron radiation sources. The participants decided to organize meetings on a regular basis (the next one taking place in Paris, probably in spring next year) to promote the application of XAS in the field of biology and to coordinate the efforts done on a European level.

M. Borowski

From 21 February to 1 April 1999, the ninth session of the HERCULES course was attended by 78 participants (out of 133 applicants). They were divided in two sessions:

- Session A: Neutron and synchrotron radiation for physics and chemistry of condensed matter .

- Session B: Neutron and synchrotron radiation for biomolecular structure and dynamics.

New lectures, devoted to the applications of neutron and synchrotron radiation techniques to the Physics of the Earth's interior and Environmental Sciences, have been introduced into the program of session A.

The program of session B was unchanged and corresponds to the contents of volume IV of the HERCULES series entitled «Structure and Dynamics of Biomolecules» (19 contributions) which should be published at the end of 1999 by Oxford University Press.

Next year, HERCULES 2000 will be the opportunity to celebrate the tenth anniversary of the course. It will be organized as usual with two parallel sessions A and B, from 27 February to 9 April 2000. A special program with a workshop devoted to recent developments and applications of neutron and synchrotron radiation will be organized at the end of the normal session for the past and present HERCULES participants. It is a significant measure of the impact of HERCULES that at the end of this 99 session about 650 scientists will have attended the course, out of about 1200 applicants since 1991.

REPORT FROM HERCULES 1999



HERCULES 2000

**HIGHER EUROPEAN RESEARCH COURSE
FOR USERS OF LARGE EXPERIMENTAL SYSTEMS**

Grenoble, 27 February – 9 April

Information:

Marie-Claude SIMPSON - Secrétaire
HERCULES
CNRS – Maison des Magistères
BP 166

F-38042 Grenoble Cedex 6 - France
Tel: +33 (0)4 76 88 79 86
Fax: +33 (0)4 76 88 79 81
e-mail: simpson@polycnrs-gre.fr
<http://www.polycnrs-gre.fr/hercules>

Workshop

«10 Years of HERCULES»

**for all HERCULES participants
devoted to recent developments and applications of
neutron and synchrotron radiation
Grenoble, 6 – 9 April 2000**

Deadline for application: 16 October 1999



EUROCONFERENCE AND NEA WORKSHOP ACTINIDE-XAS-98

During recent years the interest in applying synchrotron radiation techniques to the investigation of radionuclides and, in particular, actinides has grown rapidly. Important research topics, where a molecular-level understanding is mandatory, include the behavior of radionuclides in the environment, nuclear waste management, radiopharmaceutical chemistry, and general actinide chemistry and physics.

On 4-6 October 1998 the first Euroconference and NEA Workshop on Speciation, Techniques, and Facilities for Radioactive Materials at Synchrotron Light Sources, Actinide-XAS-98, took place at the ESRF/ILL site. Over 90 scientists came from 13 European countries, USA, and Japan. Among them were 22 young scientists with an average age of 26 who benefited from travel awards provided by the European Commission. The main objectives of Actinide-XAS-98 were:

- to introduce the type of information that can be obtained from synchrotron-based techniques to environmental and radionuclide scientists,
- to report the latest results on radionuclide/actinide work, and
- to inform on protocols which are in place for actinide research at several synchrotron storage rings throughout the world.

The first day had tutorial character and introduced several synchrotron radiation techniques. H. Nitsche described the sources of environmental contamination by radionuclides, the importance of understanding the chemical behavior of radionuclides under environmental conditions, and the role x-ray absorption fine-structure (XAFS) spectroscopy plays in these investigations. D. C. Koningsberger, J. Goulon, and A. Filipponi presented the physical principle of XAFS and related experimental and theoretical aspects. V. I. Nefedov gave an introduction to x-ray photoelectron spectroscopy (XPS). D. K. Shuh described the complementary application of XPS, near-edge x-ray absorption fine structure, and x-ray emission spectroscopy on actinide materials at energies below 2 keV. W. Matz and G. H. Lander gave tutorial



lectures on x-ray diffraction and the application of x-ray scattering to the magnetism of actinides, respectively. U. Wahlgren covered a different aspect related to XAFS studies, i.e. molecular modeling of actinide complexes in aqueous solutions.

Representatives of nearly all laboratories known world wide for using synchrotron radiation to study actinides reported on their latest results during the second day. Five invited and eleven contributed lectures and 22 poster presentations showed what sort of important structural, chemical, and physical information on technetium, uranium, neptunium, and plutonium samples can be obtained using synchrotron radiation. The majority of presentations were about XAFS studies on actinide complexes in solution, crystalline samples, and sorption of radionuclides on mineral surfaces. The discussion was focused both on basic and applied research, e.g., specially-resolved XAFS measurements of contaminated soil samples. Other speakers described investigations on actinides using XPS, x-ray magnetic circular dichroism, and x-ray tomography. Many of these results can be found in the proceedings of Actinide-XAS-98, which are being edited by N. M. Edelstein, T. Reich, and S. Sakurai and will appear as a Nuclear Energy Agency (NEA) publication in April 1999.

During the last day, participants heard short presentations about experimental stations available for actinide experiments at synchrotron light sources, their experimental

possibilities, and the procedures and regulations for safe handling of radioactive materials. These reports included the following synchrotron light sources: SSRL (P. G. Allen), ESRF (P. Berkvens), ROBL-CRG at ESRF (H. Funke), APS (L. Soderholm), Photon Factory and Spring-8 (S. Tachimori), LURE (C. Den Auwer), Daresbury Synchrotron Radiation Source (A. J. Dent), and ALS (D. K. Shuh). The conference concluded with a tour of several ESRF beamlines including ID20 (magnetic scattering), ID21 (x-ray microscopy), ID22 (x-ray fluorescence microprobe), and ID24 (dispersive EXAFS). Of special interest to many participants was the new Rossendorf Beamline (ROBL, BM20), which had just completed its first XAFS measurements of radioactive samples. The participants asked for detailed explanations of the radiochemistry safety system, the sample handling in the specially designed glove box, and the remote positioning of samples and detectors.

The conference organizers (N. M. Edelstein, C. Kunz, C. Madic, H. Nitsche, T. Reich, and S. Sakurai) thank the European Commission, OECD /NEA, ESRF, and FZR for financial support of the conference. Finally, I thank all those who contributed to making Actinide-XAS-98 a great event and an important step in the application of synchrotron radiation to radionuclide/actinide studies. It is not possible to name everyone here, but special thanks are due to M. Glückert for her invaluable help as conference secretary.

T. Reich



30TH COUNCIL MEETING

25 and 26 November 1998 in Grenoble

SCIENTIFIC MATTERS

The Council

- took note of the scientific program for the period 1999 to 2003 presented by the Management which, further to the enhancement of the radiation source and to technical developments on the chain "optics – sample handling – detectors – data handling", provides for some specific refurbishment measures such as the enhancement of materials sciences at ID11 by a further experimental station or the separation of beamlines ID12A and ID12B which presently share the same location. In addition the program addressed the development of a proper scientific life at the ESRF;
- noted the modifications of the CRG beamlines IF and FIP (construction of a second branch on FIP, dedicated to absorption spectroscopy in very dilute materials, in connection with environmental sciences and concentration of IF on surface science and interface studies) and of DUBBLE (replacement of the powder diffraction set-up by one to be used for protein crystallography) and authorized Management to implement the corresponding agreements with the CRGs involved;
- welcomed the continuation and development of the collaboration between the ESRF and the EMBL (European Molecular Biology Laboratory) and considered that the EMBL's wish for access to beam time (in recognition of its contribution)

might be dealt with in the framework of the block allocation of shifts for protein crystallography (see page 9). The Council was content that Management negotiate with the EMBL on this basis and that the results be submitted to the spring meetings of the Science Advisory Committee and the Council;

- agreed that a medium-term arrangement on the use of the ESRF be concluded with the Institute of Physics of the Czech Academy of Sciences;



- appointed a new Science Advisory Committee for the period 1999/2000 (see below).

FINANCIAL MATTERS

The Council

- approved the budget for 1999 as presented, i.e. providing for an expenditure of 428.5 million French francs and requiring Members' contribution of 400 MFF;
- took note of the Medium-Term Financial Estimates (1999-2003) presented by Management (which

however did not include any staffing or financial provision connected with the 35-hours legislation);

- noted 404 MFF (or about 61.2 million Euro) as the level of new contributions from Members to the budget for the year 2000.

INDUSTRIAL POLICY

The Council endorsed (with a minor amendment) the draft industrial policy presented by Management for further discussion by the Purchasing Committee and the Administrative and Finance Committee, and final approval by the Council. This policy describes the principal aims for links with industry and the means (sale of beam time, dedicated industrial beamlines, arrangements on transfer of know how and technology...). The Council agreed, on a temporary basis, that the income from the sale of beam time and other commercial activity be used along the lines incorporated in this draft policy.

DIRECTORATE

The Council adopted "Guidelines for selecting and appointing ESRF Directors" and noted a tentative schedule for selecting and appointing the Director General (from 2001 on), aiming at having the contract approved at the autumn 1999 meeting of the Council (see page 2).

K. Witte

NEW SCIENCE ADVISORY COMMITTEE

New members for the years 1999/2000

J. Bordas (Universitat Autònoma de Barcelona), **L. Braicovich** (Politecnico di Milano), **R. Fourme** (LURE), **H. Fuess** (Technische Hochschule Darmstadt), **P. Gillet** (ENS Lyon), **R. Hilgenfeld** (Institut für Molekulare Biotechnologie, Jena), **K. Hodgson** (SSRL, Stanford),

G. H. Lander (Institute for Transuranium Elements, Karlsruhe), **L. B. McCusker** (ETH Zürich), **S. Mobilio** (Laboratori Nazionali di Frascati), **H. Möhwald** (Max-Planck-Institut für Kolloid- und Grenz-flächenforschung, Berlin), **T. Paakkari** (University of Helsinki), **D. Raoux** (CNRS, Grenoble), **T. Rayment** (Cambridge University),

G. C. Ruocco (Universita dell'Aquila), **B. Salbu** (Norges Landbrukshøgskole, Ås), **J. M. Sanz** (Universidad Autònoma de Madrid), **G. A. Sawatzky** (Rijksuniversiteit Groningen), **D. Stuart** (University of Oxford), **D. P. Woodruff** (University of Warwick), **G. Wortmann** (Universität GH Paderborn), **T. Zemb** (CEA Saclay).



LATEST BEAM TIME REQUESTS

A total of 644 applications were submitted for the September 1998 deadline for beam time between February and July 1999, for the 29 ESRF and 7 CRG beamlines that will be operating during this period. This is slightly lower than the number received in March 1998, the Block Allocation Group scheme (see below) accounting for a nominal drop by about 85 in the number of life sciences submissions.

Following the meetings of the Review Committees at the ESRF on 22 and 23 October 1998, 358 proposals were allocated beam time totalling 5153 shifts. Of these, two new long-term projects were accepted for a period of two years. Details of the applications and allocations, per committee, are summarized in Table 1. Considered overall, some 55.6% of proposals were successful this round, compared with an average of 48% over previous rounds.

Table 2 shows the number of shifts scheduled for user experiments compared with shifts requested, per scheduling period, since the beginning of user operation in September 1994. It should be noted that the second scheduling period each year to date has been slightly shorter than the first, so that there have been proportionately fewer shifts allocated and scheduled during the second half of each year.

Finally, interested readers are reminded that the next deadline for

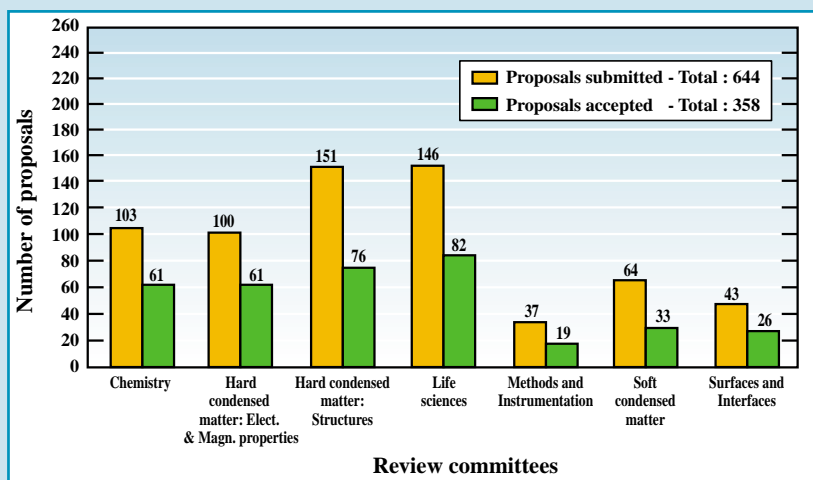


Table 1: Number of proposals and allocated beam time, per review committee, scheduling period 1999/I.

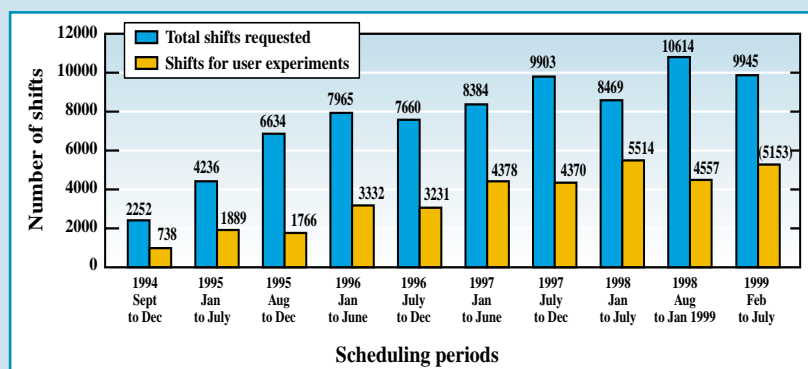


Table 2: Number of shifts of beam time requested and allocated, per scheduling period, 1994 to 1999/I.

proposals, for beam time between February and July 2000, is 1 September 1999. Further details can

be consulted on the Web at <http://www.esrf.fr>.

R. Mason

NEW MEASURES FOR THE LIFE SCIENCES USERS

In the area of life sciences, five beamlines will cater for macromolecular crystallography which constitutes the overwhelming majority of life sciences requests. These include four stations on the Quadriga beamline ID14, the MAD beamline BM14 to be transferred to ID29, ID2B where half the beam time is scheduled for macromolecular crystallography experiments and the new French CRG beamline BM30.

In parallel, measures have been taken to assist users in the area of macromolecular crystallography, and to streamline procedures. These have

been necessary in view of the dramatic increase in capacity, coupled with very rapid data collection times - frequently less than one shift - which are opening up opportunities for user groups, and at the same time placing unprecedented demands on the beamline and support staff. A possibility to test crystals prior to preparing a formal application for beam time was introduced recently. Such test experiments are fitted in between user experiments, or on buffer days, to ensure fast access. Beam time for each test is limited, normally to two hours at most. Further a Block Allocation scheme was introduced

during the second scheduling period in 1998 for macromolecular crystallography requests. A number of groups - Block Allocation Groups, or BAGs - throughout Europe, with a history of successful peer review were identified, and encouraged to group their requests for beam time. The scheduling of their beam time is also grouped, allowing these teams greater flexibility in the choice of projects and samples. At the same time, these BAGs are requested to nominate one to two persons who will be trained to provide additional help when these teams are taking beam time.



COSMETIC RECIPES AND MAKE-UP MANUFACTURING IN ANCIENT EGYPT

P. MARTINETTO^{1,2}, E. DOORYHEE¹, M. ANNE³, J. TALABOT⁴, G. TSOUCARIS² AND PH. WALTER²

1 ESRF, EXPERIMENTS DIVISION

2 LABORATOIRE DE RECHERCHE DES MUSÉES DE FRANCE, CNRS, PARIS (FRANCE)

3 LABORATOIRE DE CRISTALLOGRAPHIE, CNRS, GRENOBLE (FRANCE)

4 L'ORÉAL-RECHERCHE, CLICHY (FRANCE)

Powder x-ray diffraction, carried out at the ESRF (BM16), was used to elucidate the composition and the elaboration processes of the mineral constituents of ancient Egyptian cosmetics.

The funerary furniture discovered in Egyptian tombs, dating from between 2000 BC and 1200 BC, provides a lot of information about the customs of everyday life in Ancient Egypt [1]. Among these objects there was an abundance of toilet accessories: mirrors, hairpins, eyeliner applicators, combs or spatulas, and make-up receptacles, some of which are now preserved in the Egyptian Department of the Louvre Museum (Figure 1). Inside these 3-4000 year old containers made of marble, alabaster, wood or reed, were found cosmetic powders in an exceptionally good state of conservation. In order to decipher their composition and the

methods used in their elaboration, the organic fractions were analyzed by chromatographic techniques and the mineral content by Scanning Electron Microscopy, IRTF spectrometry and powder x-ray diffraction [2]. Standard laboratory quantitative x-ray diffraction was impeded by several factors: 1) owing to the high archaeological value of the powders, only small quantities can be extracted and analyzed; 2) the as-found cosmetics are highly absorbing mixtures of lead-based compounds; 3) most mixtures contain as many as 10 phases, i.e. the resulting diffractograms display a complex series of overlapping Bragg lines. The measurements carried

out at the ESRF (BM16) and at LURE (DW22) were able to take advantage of the high flux, the high energy and the high resolution. The Rietveld refinement method (Fullprof software package) was applied to work out the respective crystalline phase mass fractions. Taking into account the anisotropic line profile of some phases, it was possible to significantly improve the fit agreement factors (to less than 10%) and it was possible to detect quantities of minerals down to 0.5% (see Figure 2).

Two natural compounds bound with some animal grease were identified: crushed ore of black galena (PbS) and cerussite (PbCO₃). Galena is still the basic constituent of many khols traditionally used in North Africa, Asia and the Middle-East nowadays. White cerussite enters the composition of gray-to-white make-up. More surprisingly our analyses revealed the presence of two more white constituents: laurionite (PbOHCl) and phosgenite (Pb₂Cl₂CO₃). These products are very rare in nature and could not have been extracted from the mines in sufficient quantities for the preparation of the cosmetics. These products could have been formed by chemical alteration and ageing, assuming the original content of the make-up receptacles had been in contact with carbonated and chlorinated waters. However, no clear trace and no evidence of such alteration processes could be found in any of the 49 recipients.

Therefore one major conclusion of this work is that laurionite and phosgenite were intentionally manufactured by the Egyptians. The texts of Pliny the Elder and Dioscorides (first century AD) report on a number of medical recipes. In particular some of them refer to the use of lead oxide, that

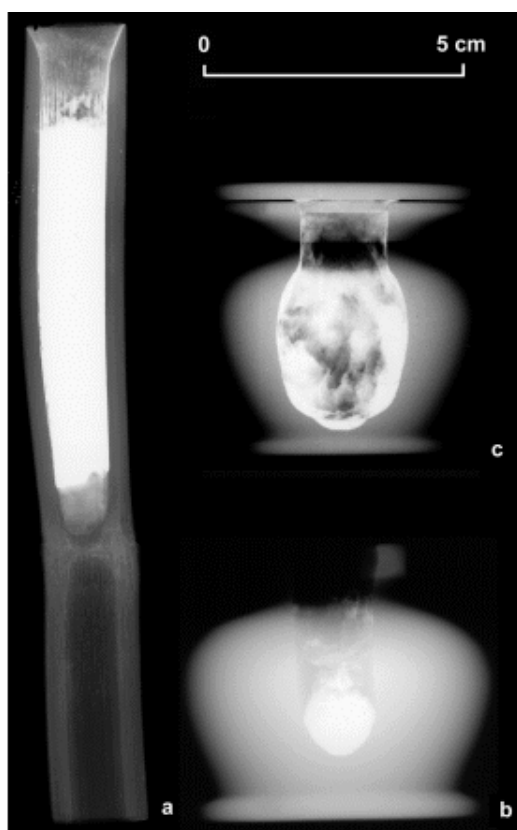


Fig. 1: X-ray radiography of different makeup receptacles from the Egyptian collections of the Louvre Museum. The white areas show the distribution of the X-ray absorbing lead powders present in the make-up. (a) reed case E, still full of makeup. (b) alabaster recipient with a fabric lid. (c) alabaster recipient and cover. It contains a small amount of makeup attached on the inner wall.



was ground and diluted into salted and sometimes carbonated (natron) water. This wet process was mimicked in the laboratory. By maintaining the solution at a neutral pH, a slow reaction yields white precipitates of either laurionite or phosgenite. This is the first indication that wet chemistry has been practiced since 2000 BC.

Why should these white lead derivatives PbOHCl and $\text{Pb}_2\text{Cl}_2\text{CO}_3$ be added to black PbS , since white cerussite PbCO_3 was sufficient to vary and tune the cosmetics tint from black to white? One should consider that since the earliest periods of Egyptian history, the cosmetics have been intensively used not only for aesthetic purposes, but also for their therapeutic and magic or religious properties. The Greco-Roman texts mention that the white precipitates synthesized from PbO are good for eye and skin care. These lead compounds could be used as a bactericide and as a protection for the eye against exposure to the sun's rays.

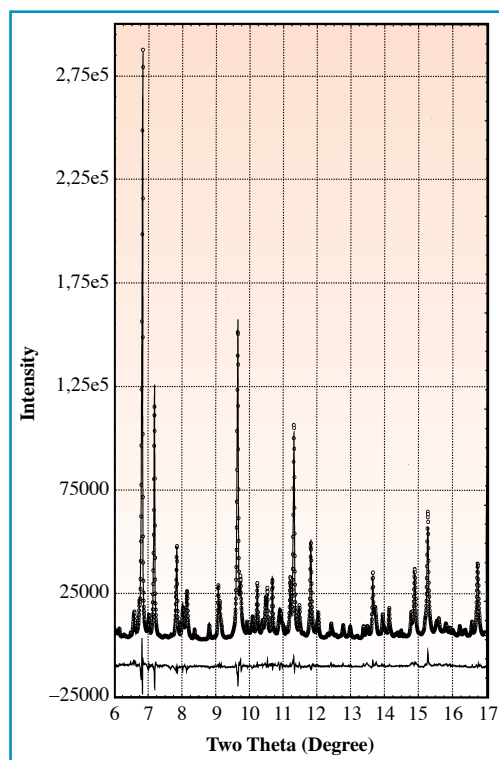
In addition, the diffraction peak profiles are also being analyzed, comparing strain and crystallite size broadening effects in archaeological, synthetic and natural powders [3]. Given the small instrumental broadening of BM16 ($0.005^\circ 2\theta$), a preliminary peak breadth analysis shows that the PbS ore present in the cosmetics was ground and sorted

Fig. 2: Powder pattern measured on BM16 at $\lambda = 0.35 \text{ \AA}$ of an archaeological sample dated from the Tutankhamon reign: observed (o), calculated (—) patterns and difference curve.

according to grain size. The resulting granulometry of galena provided the make-up with the expected texture and its metallic brightness. By contrast the Bragg line broadening of PbOHCl and $\text{Pb}_2\text{Cl}_2\text{CO}_3$ is free from any strain: this suggests that they have been directly synthesized as fine powders and have not been prepared by crushing. Therefore the x-ray line broadening related with the crystallographic microstructure can help to determine the origin and the process of elaboration of archaeological powders. ■

REFERENCES

- [1] A. Lucas, J.R. Harris, "Ancient Egyptian materials and industries" (Edwards Arnold Ltd., London) (1963).
 [2] Ph. Walter, P. Martinetto, G. Tsoucaris, R. Brénioux, M.A. Lefebvre, G. Richard,



J. Talabot, E. Dooryhee, "Manufacturing cosmetics in ancient Egypt", *Nature* 397, 483-484 (1999).

[3] P. Martinetto, M. Anne, E. Dooryhee, Ph. Walter, "Analysis of x-ray diffraction line profile of galena powders: a clue to some practices of mineral crushing in ancient Egypt", *Proceedings of the 6th European Conference on Powder Diffraction (EPDIC6), Materials Science Forum* (1998).

VACANCIES AT THE ESRF ON 30 MARCH 1999

	Ref	Subject	Deadline
SCIENTIST	9907	For the construction of a dedicated X-ray microbeam end-station.	15/04/99
	2163	For the Surface Science group ID32	10/05/99
	2119	For the Magnetic Scattering Beamline ID20	17/05/99
	2185	For the X-ray Absorption Spectroscopy group ID12B	17/05/99
<i>Previous postdoctoral experience with synchrotron radiation is essential.</i>			
POST-DOC	PDID15B-1	For the High Energy Inelastic X-ray Scattering beamline ID15B	03/05/99
	PDID26	For the EXAFS and related spectroscopies on beamline ID26	07/05/99
	PDID13-2	For the Microfocus beamline ID13	10/05/99
TECHNICIAN POSITIONS	6532	Technician in the Central Mechanical Workshop	16/04/99
	6527	Technician in the Survey and Alignment Group	16/04/99
	2525	Technician for the Inelastic X-ray Scattering beamline ID16	30/04/99

If you are interested, please send us a fax (+33 (0) 4 76 88 24 60) or an e-mail (recruitm@esrf.fr) with your address, and we will provide you with an application form. You can also print out an application form on the World Wide Web <http://www.esrf.fr>



FIRST OBSERVATION OF A MAGNETIC SPECKLE PATTERN BY COHERENT X-RAY SCATTERING AT THE URANIUM M_{IV} EDGE

F. YAKHOU¹, A. LÉTOUBLON², F. LIVET², M. DE BOISSIEU², F. BLEY² AND C. VETTER¹

¹ ESRF, EXPERIMENTS DIVISION

² LTPCM-ENSEEG, UMR-CNRS/INPG/UJF N°5614, ST MARTIN D'HÈRES (FRANCE)

The availability of high fluxes of coherent hard x-rays has opened up new fields of investigations on disordered systems, through the analysis of the random diffraction or "speckle" patterns. A promising application is the study of the disorder inherent to domain formation in magnetic systems.

Taking advantage of the high quality focusing optics of the ID20 beamline and the huge enhancement of the magnetic scattering amplitude when the energy is tuned to the M-edges of uranium (< 4 keV), we were able to record a magnetic speckle pattern from the antiferromagnetic phase of a UAs sample.

When scattered by coherent incident radiation, any disordered material introduces random phase-shifts that result in a strong modulation of the average diffraction pattern yielding the graininess characteristic of a speckle pattern. Each such pattern is related to the exact spatial arrangement of the disorder and to the coherence properties of the incident radiation. It will evolve together with both these features, making the knowledge of the properties of the incident radiation essential to retrieve meaningful information on the sample itself.

Extracting the exact arrangement of the sample from a static speckle pattern, though theoretically possible, is in practice a daunting task. Much of our experimental work has been dedicated to intensity fluctuation spectroscopy by analyzing the time correlation of the intensity on a single point of a speckle pattern, thus giving information on the underlying dynamics with nearly atomic resolution and frequencies ranging in practice from 10^{-3} Hz to 10 Hz.

Antiphase domain structure in Cu_3Au , equilibrium critical fluctuations in Fe_3Al , brownian motion of gold colloids in glycerol, dynamics of block copolymer micelles have been successfully addressed by coherent scattering techniques in the 8 keV energy range [1], where a high flux of coherent x-rays can be "easily" obtained. A new exciting domain of applications will be the study of magnetic domains.

Because of crystal symmetry, domain formation is inherent to most types of magnetic ordering but little is known up to now on domain size and arrangement. A speckle pattern from a magnetic system should prove of considerable interest in this respect. Since the main difficulty lies in the extreme weakness of the magnetic signal, UAs was chosen as a test system for which advantage can be taken from the huge enhancement of the magnetic intensity through a resonant process at the uranium M_{IV} absorption edge (3.73 keV). The unavoidable counterpart is a lower flux at the sample due to higher absorption by windows. UAs has the crystal structure of NaCl with a lattice parameter $a_0 = 5.766 \text{ \AA}$ and orders at $T_N = 127 \text{ K}$ in a type-I antiferromagnetic structure with alternating ferromagnetic sheets stacked

along the c-axis.

A $20 \mu\text{m}$ collimating pinhole selected the coherent fraction of a 3.73 keV beam from the first harmonic of two phased 42 mm period undulators, its spectral width given by the 1.3×10^{-4} bandwidth of a Si (111) double crystal monochromator. A secondary set of slits of adjustable aperture placed after the optics, 3 meters from the pinhole, acted as the effective source, thus avoiding any spoiling of the coherence by optical elements. The second crystal of the monochromator and the second mirror were used to focus the beam horizontally and vertically respectively, down to $350 \times 80 \mu\text{m}^2$ in the pinhole plane. The resulting integrated flux through the $20 \mu\text{m}$ pinhole was as high as 7.10^7 ph/s at 180 mA ring current with a $60 \times 60 \mu\text{m}^2$ opening of the secondary

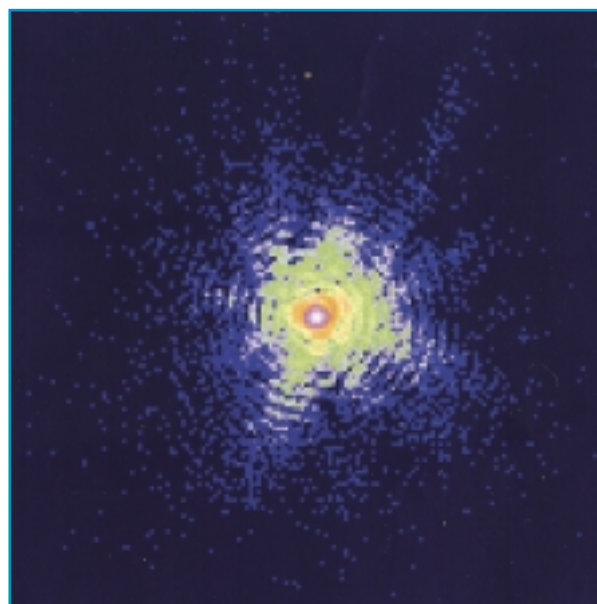


Fig. 1: Fraunhofer diffraction pattern from a $10 \mu\text{m}$ pinhole at 3.73 keV. The fringes are visible up to the tenth order, indicating the high degree of coherence of the illuminating radiation.

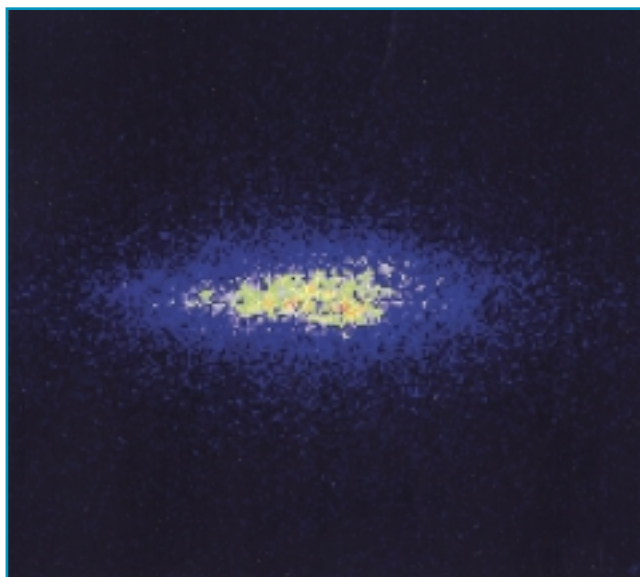


Fig. 2: Speckle pattern from magnetic domains in the type-I antiferromagnetic phase of UAs, at the uranium M_{IV} resonance (3.73 keV). Horizontal and vertical cuts are displayed in Fig. 3.

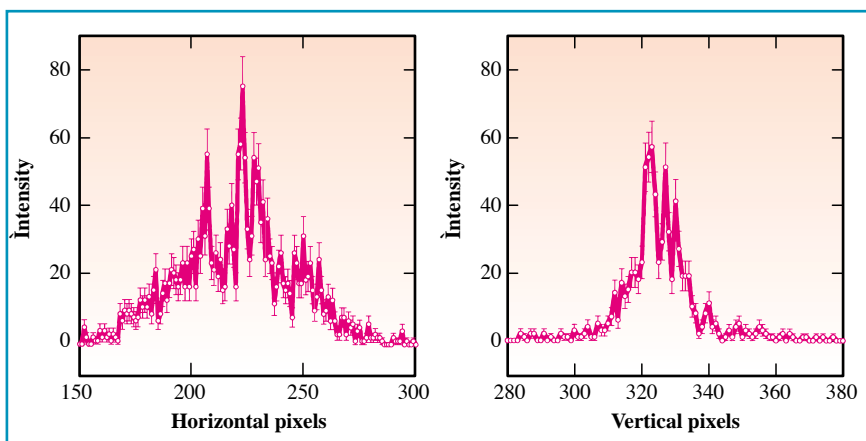


Fig. 3: Horizontal and vertical cuts through the speckle pattern of Fig. 2. The error bars correspond to Poisson statistics and cannot account for the raggedness in the scattering.

slits. It is worthwhile noting that we could obtain up to 7.10^8 ph/s at 140 mA current through a $10 \mu\text{m}$ pinhole and $60 \times 60 \mu\text{m}^2$ slits at 7.6 keV, with a 48% degree of coherence (β) at small angle, which is by far the highest and best coherent flux achieved up to now.

Both a standard Bicorn scintillation detector and a Princeton Instruments direct illumination CCD chip with 384×576 $22 \mu\text{m}$ square pixels could be used as detectors, 1.8 m away from the sample. The CCD camera was used as a 2D photon counter by applying a droplet algorithm [2] that could identify individually each photon reaching the camera.

The coherence properties of the beam were retrieved from the statistical analysis of the static speckle pattern produced by a silica gel following an earlier paper [2]. β , as given by the contrast of the speckle pattern, was found to be around 50%,

though evolving with time down to 30% within half an hour, indicating instabilities in the experimental set-up that we suspect to come from temperature variations in the experimental hutch. The Fraunhofer diffraction pattern of a $10 \mu\text{m}$ pinhole at 3.73 keV is displayed on Figure 1. The good contrast of the fringes up to the tenth order is a clear sign of the high coherence of the illuminating beam.

The $5 \times 5 \times 2 \text{ mm}^3$ UAs sample was oriented with a [001] cleaved surface and put in a cryostat with $2 \times 500 \mu\text{m}$ thick inner Be windows and $2 \times 125 \mu\text{m}$ thick outer Kapton windows, giving a total 2% transmission at 3.73 keV. Because of practical limitations in the detector 2θ angle, the crystal orientation and intensity optimization were done at 3.75 keV. The sample was then cooled down to 100 K, in the magnetically ordered phase. By tuning the energy to the maximum of the

resonance we achieved 60 counts per second at peak maximum on the (001) antiferromagnetic reflection from a $\approx 40 \mu\text{m}$ single grain, a result somewhat expected from previous non-coherent experiments on the very same sample. A time-series of 181 summed up 10 second each acquisition frames is represented on Figure 2. A speckle structure is clearly visible. Vertical and horizontal cuts through the image are displayed in Figure 3, with error bars corresponding to Poisson counting statistics that clearly cannot account for the raggedness in the scattering.

Because of crystal symmetry, one would not expect the diffraction pattern to be anisotropic. The apparent $1:\approx 4$ anisotropy of the scattering can be accounted for by a considerable smearing of the (001) reciprocal lattice node along the scattering vector due to strong absorption effects. For the given experimental geometry the 2D CCD image can be viewed as a planar cut in the reciprocal space perpendicular to the diffracted wavevector, thus at an angle $\theta_{001} = 15^\circ$ to the scattering vector. That would result in a $\cos\theta:\sin\theta$ anisotropy of the diffraction pattern.

Using the high coherent flux at 3.73 keV that was obtained on the ID20 beamline, we have demonstrated the feasibility of coherent scattering experiments on magnetic systems that should give a unique insight on the physics of magnetic domains. The even higher flux obtained at 7.6 keV should allow investigations at the L absorption edges of rare-earth compounds with weaker resonances, opening up this new field to a wide variety of magnetic systems. ■

REFERENCES

- [1] M. Sutton *et al*, *Nature* 352 (1991); S. B. Dierker *et al*, *PRL* 75 (1995); S. G. J. Mochrie *et al*, *PRL* 78 (1997); S. Brauer *et al*, *PRL* 74 (1995) and F. Bley *et al*, *Acta Cryst.* A51 (1995)
- [2] F. Livet *et al*, *J. Synchrotron Rad.* 5 (1998) and F. Livet *et al*, submitted to *J. Synchrotron Rad.* (1998)

ACKNOWLEDGEMENTS

Scientific and technical help from C. Detlefs, G. Grübel, R. Caudron, R. Chagnon, W. Neubeck, D. Mannix and B. Caillot is greatly acknowledged.

X-RAY RESONANT SCATTERING AND ORBITAL ORDER IN V_2O_3

L. PAOLASINI¹, C. VETTIER¹, F. DE BERGEVIN², D. MANNIX^{1,3}, W. NEUBECK¹, A. STUNAU¹,
F. YAKHOU¹, J. M. HONIG⁴ AND P. A. METCALF⁴

1 ESRF, EXPERIMENTS DIVISION

2 LABORATOIRE DE CRISTALLOGRAPHIE, CNRS, GRENOBLE (FRANCE)

3 EUROPEAN COMMISSION, JRC, INSTITUTE FOR TRANSURANIUM ELEMENTS, KARLSRUHE (GERMANY)

4 DEPARTMENT OF CHEMISTRY, PURDUE UNIVERSITY, WEST LAFAYETTE, INDIANA (USA)

X-ray resonant scattering has provided unambiguous evidence for the appearance of orbital order in V_2O_3 confirming the hypothesis made twenty years ago [1] to explain the complex behavior of this material. Our results demonstrate that the resonant x-ray methods can be exploited to extract information on the electronic orbital degrees of freedom in solids.

In 3d transition metal compounds, the unscreened 3d electrons take part in the chemical bonding and contribute to the electronic and magnetic properties. This leads to a delicate interplay between the magnetic interactions and the chemical bond configurations. In particular, the electronic spin and orbital degeneracies can induce very intricate associations of electronic and magnetic states. If it is relatively easy to obtain immediate evidence for spin or charge ordering through the usual scattering techniques or local probes, the direct observation of orbital order is hindered by the lack of sensitivity of the standard scattering methods.

Resonant x-ray scattering (RXS) is a technique which is used to label chemical species and electronic shells. When the incident photons have an energy close to an absorption edge of a constituent of the material, scattering arising from this particular species is enhanced. Resonant scattering arises from coherent processes determined by the local point symmetry. Two well-known examples are Templeton scattering (TS) and magnetic resonant scattering (MRXS). In the case of MRXS, it is the onset of a local magnetic moment that breaks the symmetry, whereas low point symmetry of a site in a crystal gives rise to TS.

The lowering of symmetry can be brought about by the ordering of electronic orbitals. When electronic configurations are degenerate, the crystal may restructure by removing the degeneracy of the orbital occupancy in order to minimize its total free energy. On the one hand, this leads to lattice distortions (cooperative Jahn-Teller effect) which can be observed by usual scattering methods; on the other hand, the uneven occupation of equivalent electronic orbitals opens new channels for resonant scattering [2,3] even in the absence of lattice distortions.

We have used the RXS method to bring to light the onset of long range orbital order in V_2O_3 . This material exhibits a rich phase diagram [4], involving metallic and insulating phases with different magnetic states. Twenty years ago, the long range order of the 3d

orbital occupancy was invoked to account for the complex magnetic structure [1] and excitation spectrum but so far there has been no direct evidence for such a new periodicity in V_2O_3 crystals.

Encouraged by theoretical predictions, we have undertaken a search for the onset of orbital order in V_2O_3 . This compound exhibits a para-antiferromagnetic transition which is strongly first-order and destructive. In order to mitigate these effects, we have selected a Cr-doped sample whose shape and dimensions (1.0 x 0.8 x 0.05 mm³) were optimized to ensure that the single crystal would survive through the phase transition. The RXS experiments were performed at the ID20 Magnetic Scattering undulator beamline at the ESRF around the vanadium K-edge at 5.476 keV.

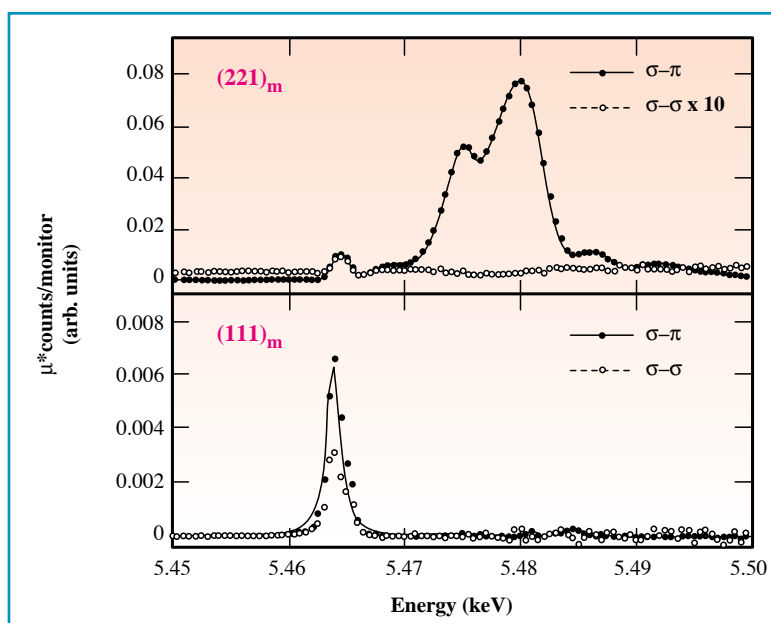
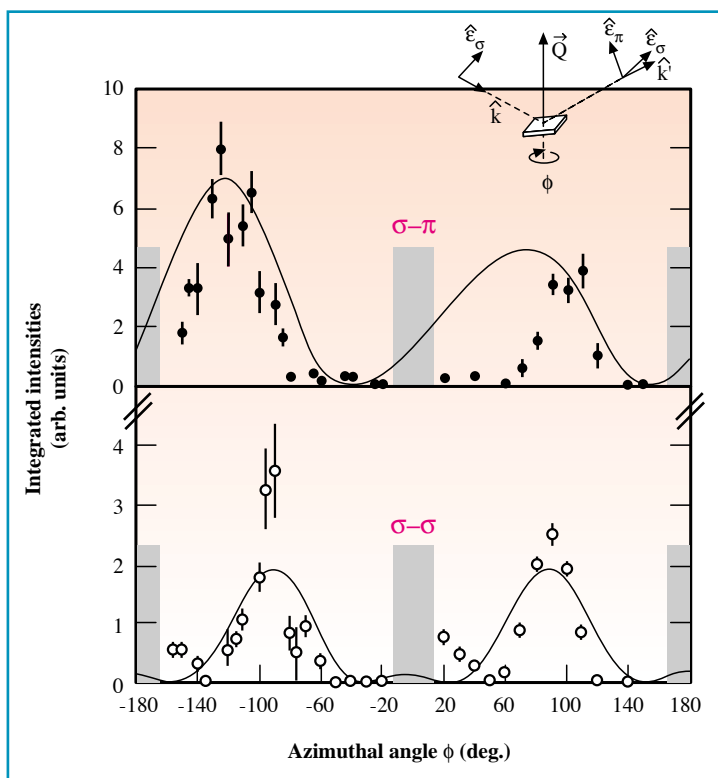


Fig. 1: Energy dependence of the (221)_m magnetic reflection (top panel) and the (111)_m orbital peak (bottom panel) at $T = 100$ K for the two polarization channels $\sigma\text{-}\sigma$ and $\sigma\text{-}\pi$.



Polarized integrated intensities of the (111) orbital reflection measured at different azimuthal angles for a photon energy of 5.464 keV. The shaded areas indicate zones that were inaccessible due to the sample mount.

Below the Néel temperature $T_N = 181$ K, two new and distinct sets of Bragg reflections can be observed. The first set of reflections corresponds to the antiferromagnetic order: their position in reciprocal space coincides with the magnetic propagation wavevector and the polarization analysis of the scattered intensities confirms their magnetic character. The variation of the intensity of one of these reflections with photon energy is displayed in Figure 1 (top panel). Two resonances can be observed at energies above and below the vanadium K-edge on top of the non-resonant magnetic scattering. The second set of reflections can be detected only at the low energy resonance (5.464 keV) over a narrow energy window of 1.6 eV (Figure 1 lower panel). These new Bragg peaks are associated with the long range order of orbital ordering in V_2O_3 for two reasons: i) the energy and polarization dependence denotes the vanadium d-electrons as the origin of the scattering, ii) the azimuthal dependence (Figure 2) of the resonant intensity follows predictions by Fabrizio *et al.* [2]. Furthermore, the observed propagation wavevector was suggested by Castellani [1] to account for the magnetic couplings in V_2O_3 . We have also monitored the temperature dependence of the magnetic and orbital responses in the Cr-doped V_2O_3 sample: the two order parameters

follow similar temperature dependences below $T_N = 181$ K as determined from susceptibility measurements. Such behavior illustrates the intimate coupling between orbital order and magnetic order in V_2O_3 . Our experimental observation of long range ordering in the occupancy of 3d orbitals in V_2O_3 confirms predictions made twenty years ago and underlines the central role of orbital occupancy in electronic properties of solids.

Fruitful discussions with M. Altarelli of the ESRF were highly appreciated. We acknowledge the help of the DRFMC/SPSMS laboratory at CEA-Grenoble for the sample preparation and Laboratory Louis Néel CNRS-Grenoble for the sample characterization. ■

REFERENCES

- [1] C. Castellani, C.R. Natoli and J. Ranninger, *Phys. Rev. B* 18, 4945 (1978); *ibid. Phys. Rev. B* 18, 4967 (1978); *ibid. Phys. Rev. B* 18, 5001 (1978).
- [2] M. Fabrizio, M. Altarelli and M. Benfatto, *Phys. Rev. Lett.* 80, 3400 (1998); *Phys. Rev. Lett.* 81, E4030 (1998).
- [3] Y. Murakami *et al.*, *Phys. Rev. Lett.* 80, 1932 (1998); Y. Murakami, *et al.*, *Phys. Rev. Lett.* 81, 582 (1998).
- [4] D.B. McWhan *et al.*, *Phys. Rev. Lett.* 23, 1384 (1969); *Phys. Rev. B* 2, 3734 (1970), *Phys. Rev. Lett.* 27, 941 (1971); *Phys. Rev. B* 7, 1920 (1973).



DETERMINATION OF THE INFINITE FREQUENCY SOUND VELOCITY IN THE GLASS-FORMER *ORTHO*-TERPHENYL

G. MONACO¹, C. MASCIOVECCHIO², G. RUOCCO¹ AND F. SETTE²

¹ UNIV. DI L'AQUILA AND ISTITUTO NAZIONALE DI FISICA DELLA MATERIA, L'AQUILA (ITALY)

² ESRF, EXPERIMENTS DIVISION

The high-frequency dynamics of the glass-former *ortho*-terphenyl is studied here in the glass transition region. Inelastic X-ray Scattering (IXS) is used to determine the dynamic structure factor $S(Q, \omega)$ in presence of relaxation processes, in a Q regime which is not accessible to other techniques, namely Brillouin Light Scattering and Inelastic Neutron Scattering.

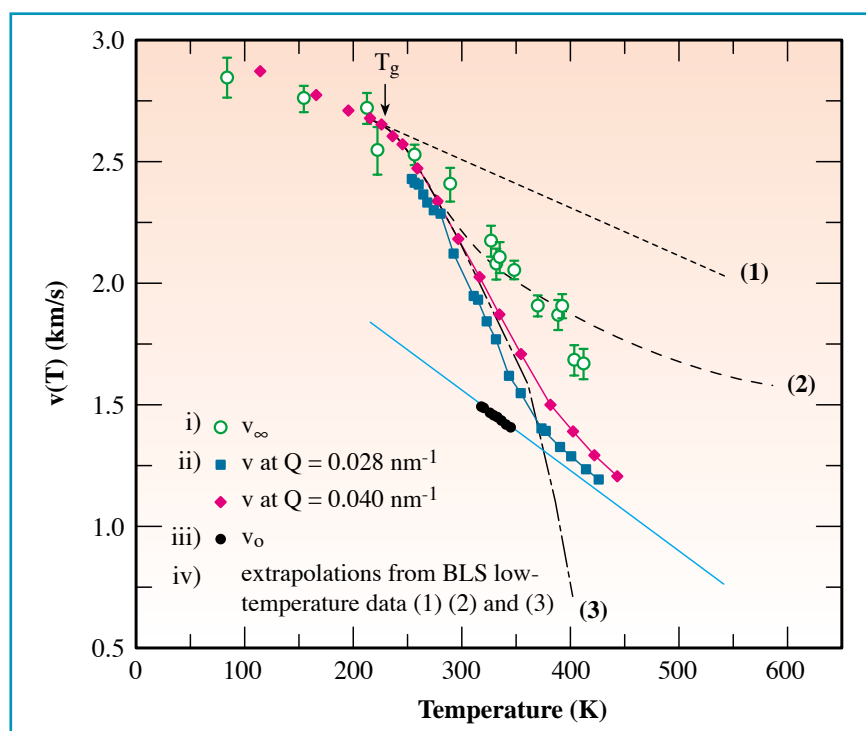
Simple liquids undergoing the glass transition, like the organic glass-former *ortho*-terphenyl studied in the present paper, are characterized by the so-called α (structural) relaxation, whose timescale $\tau_\alpha(T)$ is strongly temperature dependent. Due to this relaxation, the speed of the longitudinal waves propagating at temperature T with wavevector Q , $v(Q, T)$, presents a transition from a low-frequency ($\omega = 2\pi\nu \ll 1/\tau_\alpha(T)$) adiabatic value, $v_0(T)$ to the high frequency ($\omega = 2\pi\nu \gg 1/\tau_\alpha(T)$) purely elastic value, $v_\infty(T)$. The specific distribution of relaxation times, as well as $v_0(T)$ and $v_\infty(T)$, are the essential parameters governing the dispersion of the sound waves excitation energies and, therefore,

their experimental determination has always received great attention. The condition $\omega \ll 1/\tau_\alpha(T)$ can be met by low frequency spectroscopies, like ultrasonic ones; thus $v_0(T)$ can be measured in a wide temperature range, from the liquid phase almost down to the calorimetric glass transition temperature, T_g . The determination of $v_\infty(T)$ is much more difficult. Brillouin Light Scattering (BLS) methods detect the sound wave speed at about 10 GHz, and correspondingly determine $v_\infty(T)$ only in the glass and in the deeply under-cooled liquid where $\tau_\alpha \geq 10^{-11}$ s. The lack of information on $v_\infty(T)$ in the liquid region is currently covered by different extrapolation schemes of the low-temperature data.

The recent development of the Inelastic X-ray Scattering (IXS) technique allows to study the dynamic structure factor $S(Q, \omega)$ in a Q regime accessible neither to BLS (for which $Q \approx 0.05 \text{ nm}^{-1}$) nor to Inelastic Neutron Scattering (due to kinematic limitations). This gives the possibility to measure the dispersion relation of acoustic excitations, $\Omega(Q)$, up to frequencies where the condition $\Omega(Q) \gg 1/\tau_\alpha$ is verified in the liquid state. The quantity $v_\infty(T)$ can then be derived as the $Q \rightarrow 0$ limit of $v(Q, T) = \Omega(Q)/Q$.

In this study we performed Q - and T -dependent IXS measurements aiming to determine the temperature dependence of $v_\infty(T)$ in *ortho*-terphenyl, a typical fragile

Fig. 1: Temperature dependence of different sound velocities in *ortho*-terphenyl:
i) $v_\infty(T)$ derived from IXS measurements (open circles). ii) $v(T)$ derived from BLS measurements at $Q \approx 0.028$ (full squares) and 0.04 (full diamonds) nm^{-1} . iii) $v_0(T)$ derived from ultrasonic measurements (dots) and linearly extrapolated on a wider temperature region (solid line). iv) $v_\infty(T)$ extrapolated in the liquid from low-temperature BLS data assuming: (1) a linear extrapolation from the glass values of v_∞ (dotted line), (2) a linear dependence of the compliance $J_\infty(T)$ (dashed line) extrapolated from its values at temperatures slightly above T_g , and (3) a linear dependence of the elastic modulus $M_\infty(T)$ (dot-dashed line) extrapolated from its values at the same temperatures as $J_\infty(T)$.





glass forming system, in a temperature range covering the glass and the liquid phases. The values obtained for $v_\infty(T)$ are shown as open circles in Figure 1 and are compared to literature data of : i) $v_0(T)$ as measured by ultrasonic methods (dots) and ii) $v(Q, T)$ as measured by BLS at $\approx 0.04 \text{ nm}^{-1}$ (full diamonds) and $\approx 0.028 \text{ nm}^{-1}$ (full squares). The BLS results report the typical S-shape evolution due to the structural α relaxation, and $v(Q, T)$ makes the transition from v_∞ in the glass to a plateau in the high-temperature liquid. In the glass, where $v(Q)$ is expected to coincide with $v_\infty(T)$, there is good agreement between the IXS and BLS $v(Q)$ values. Such a result implies that in the glass region, the procedure used to extract v_∞ from the IXS data is reasonable.

Therefore, there is confidence that also in the liquid, i.e. in a temperature range not accessible before, the values obtained for v_∞ are meaningful. They are reported in Figure 1 together with three extrapolation schemes, typically utilized to infer v_∞ from low-temperature BLS data. The dotted line is obtained from v_∞ in the glass, linearly extrapolated in the liquid. Compared to the IXS determination, v_∞ is overestimated. The dashed line is obtained assuming a linear temperature dependence of the compliance $J_\infty \approx 1/\rho v_\infty^2(T)$, where ρ is the mass density. The dot-dashed line, on the other side, assumes a linear temperature dependence to the elastic modulus $M_\infty \approx \rho v_\infty^2(T)$. These last two extrapolations give both a good estimate of $v_\infty(T)$ at temperatures slightly higher

than the glass transition temperature T_g . Only the estimate based on the temperature dependence of J_∞ , however, is capable to give $v_\infty(T)$ values very similar to those obtained by IXS in the whole considered temperature range.

In summary, we have shown that it is possible to determine the infinite frequency sound velocity $v_\infty(T)$ from the high frequency dispersion relation measured by IXS. The knowledge of this parameter will allow better modelling of the $S(Q, \omega)$ in presence of relaxation processes, and, therefore, to get more reliable values of the relaxation times. ■

REFERENCE

G. Monaco, C. Masciovecchio, G. Ruocco and F. Sette, Phys. Rev. 80, 2161 (1998)

RADIATION TRAPPING IN RESONANT NUCLEAR SCATTERING OF X-RAYS

A.I. CHUMAKOV¹, J. METGE¹, A.Q.R. BARON¹, R. RÜFFER¹, YU.V. SHVYD'KO², H. GRÜNSTEUDEL^{3,1} AND H.F. GRÜNSTEUDEL¹

¹ ESRF, EXPERIMENTS DIVISION

² INSTITUT FÜR EXPERIMENTALPHYSIK, UNIVERSITÄT HAMBURG, HAMBURG (GERMANY)

³ INSTITUT FÜR PHYSIK, MEDIZINISCHE UNIVERSITÄT ZU LÜBECK, LÜBECK (GERMANY)

Radiation trapping is a well-known phenomenon in the resonant scattering of visible light by atoms. A resonant photon emitted in the interior of a gas has only a small chance of leaving the enclosure directly. Due to the high resonance cross-section, it is repeatedly absorbed and re-emitted by atoms, so that the escape of the photon from the enclosure takes place only after a large number of scattering events. The decay of atomic fluorescence may be many times longer than the natural lifetime. For instance, due to radiation trapping it takes $\sim 10^6$ years for visible light to penetrate from the solar center to its surface. In industry a proper account of radiation trapping is important for the production of mercury lamps.

So far radiation trapping was known only for visible light from atomic transitions. We observed radiation trapping of hard x-rays with a wavelength of more than three orders of

magnitude shorter, namely with the 14.413 keV radiation originating from the decay of the first excited state of the ^{57}Fe nucleus. The nuclei were excited by a short pulse of synchrotron radiation, and then the intensity of the 6.4 keV fluorescent radiation produced by nuclear internal conversion was measured as a function of time after the pulse excitation. The time distribution of nuclear de-excitation showed the expected exponential decay, however, the decay time was longer than the natural lifetime.

Figure 1 shows the time evolution of incoherent scattering from the polycrystalline ^{57}Fe foil. On the logarithmic scale it is a straight line in the time range of ~ 1 ms and over 3 decades of intensity, clearly displaying an exponential decay. The decay time of 152 ± 1 ns, obtained from the fit with an exponent and a constant background, differs significantly from the natural

lifetime $\tau_0 = 141.1$ ns. For comparison, the natural lifetime was measured with a solution of ferrocene in dibutylphthalate (Figure 1).

In order to understand the origin of the longer decay we have examined the dependence of the decay time on several parameters: the Lamb-Mössbauer factor, the sample structure, and the abundance of resonant nuclei. The most significant dependence was found in the case of the Lamb-Mössbauer factor. The results are explained with a model based on spatially incoherent multiple resonant nuclear scattering. Taking into account the first and the second re-scattering events, the time evolution of incoherent scattering can be approximated by an exponential decay with a modified lifetime $\tilde{\tau}_0$:

$$\tilde{\tau}_0 = \frac{\tau_0}{1 - f_{LM} (\Gamma_R / \Gamma_\Sigma)}$$

where f_{LM} is the Lamb-Mössbauer factor (recoilless fraction of scattering), Γ_R and Γ_Σ are the radiative and the total width of the nuclear level.

Along with slowing down the emission of the 6.4 keV fluorescent radiation, radiation trapping suppresses the yield of the resonant 14.413 keV photons, because they are converted into fluorescent radiation in every re-scattering event. We observed that the relative yield of the resonant 14.4 keV photons from a thick sample is ~ 4 times less than expected for an isolated nucleus. ■

REFERENCE

A.I. Chumakov, J. Metge, A.Q.R. Baron, R. Ruffer, Yu.V. Shvyd'ko, H. Grünsteudel, H.F. Grünsteudel, *Phys. Rev. B* 56 (1997) 8455.

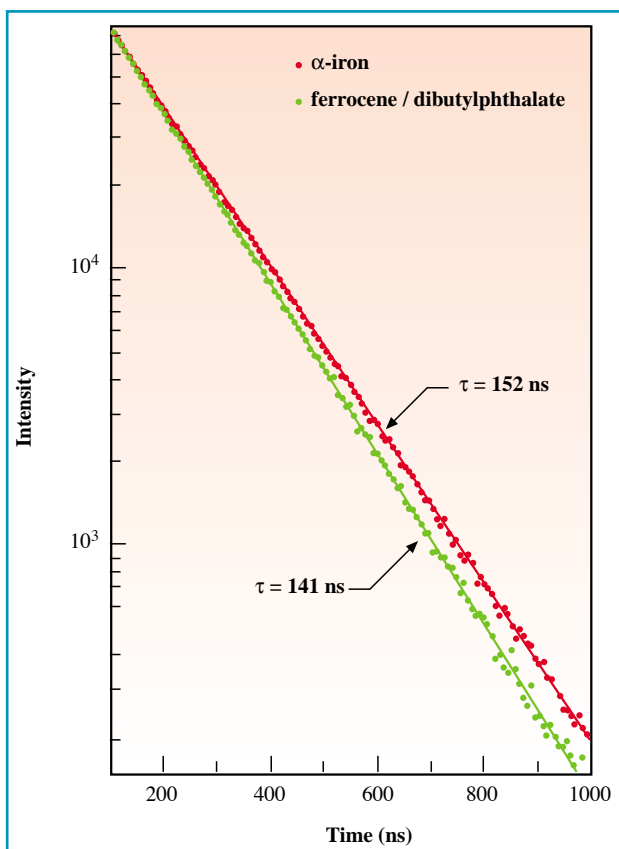


Fig. 1: Time evolution of incoherent nuclear scattering by ^{57}Fe sample (red circles) and by a solution of ferrocene in dibutylphthalate (green circles). The corresponding Lamb-Mössbauer factors are 0.80 and 0.00. Solid lines are the exponential fits to the experimental data with the decay time $\tau_{exp} = 152 \pm 1$ ns for iron and $\tau_{exp} = 141 \pm 1$ ns for ferrocene / dibutylphthalate.

ANGULAR RESOLVED DENSITY OF PHONON STATES

A.I. CHUMAKOV¹, R. RÜFFER¹, A.Q.R. BARON¹, H. GRÜNSTEDEL^{1,2}, H.F. GRÜNSTEDEL¹ AND V.G. KOHN³

¹ ESRF, EXPERIMENTS DIVISION

² INSTITUT FÜR PHYSIK, MEDIZINISCHE UNIVERSITÄT ZU LÜBECK, LÜBECK (GERMANY)

³ RUSSIAN RESEARCH CENTER "KURCHATOV INSTITUTE", MOSCOW (RUSSIA)

Inelastic nuclear absorption of synchrotron radiation has proven to be a new method for studying lattice dynamics. So far polycrystalline, amorphous and fluid samples were investigated where one gets the information on lattice dynamics in an integral form, i.e. the modes of vibrations along various directions are averaged. Here we measure separately the frequency distribution of lattice vibrations along different crystallographic directions.

We have measured the energy spectra of inelastic absorption of 14.4 keV synchrotron radiation in a ferric borate $^{57}\text{FeBO}_3$ single crystal for several polar angles θ and azimuthal angles φ between the incident x-ray beam and the [111] axis (Figure 1). The

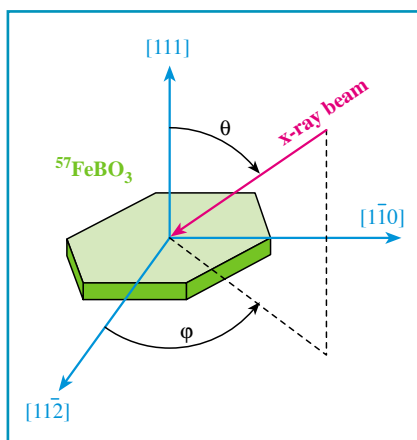
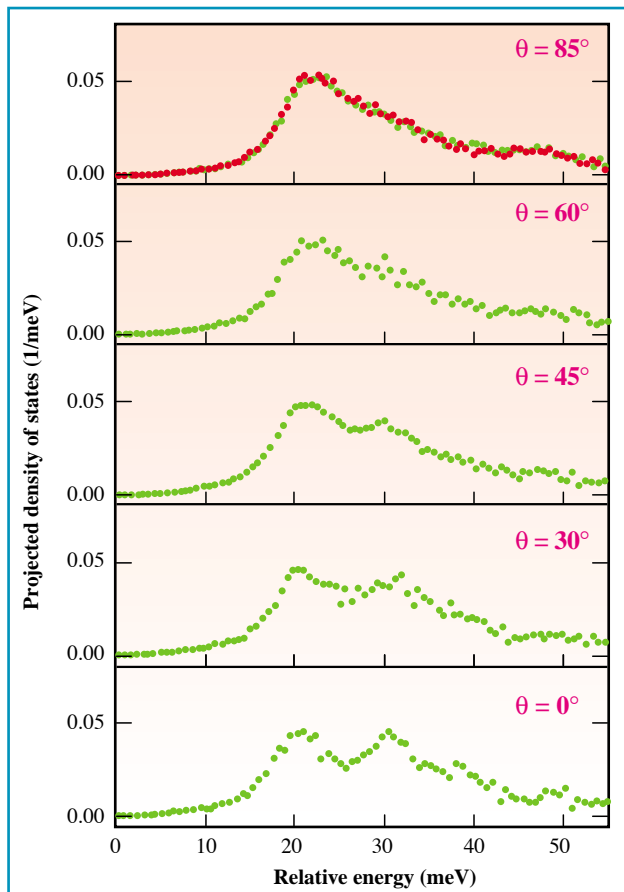


Fig. 1: Orientation of the incident x-ray beam relative to the crystal.

frequency distributions of lattice vibrations along these directions (i.e., projected densities of phonon states) were derived and the Lamb-Mössbauer factors for each case were calculated.

Derived projected densities of states are shown in Figure 2. They give the frequency distribution of lattice vibrations, weighted by the projection of the phonon polarization vector to the direction of the x-ray beam. The densities of phonon states show a pronounced dependence on the polar angle. When the polar angle is high ($\theta = 85^\circ, 60^\circ$) the densities of states

Fig. 2: The projected densities of phonon states along several crystallographic directions. The polar angles θ for various directions are indicated in the Figure. The data for the azimuthal angle $\varphi = 90^\circ$ are shown with green circles and for $\varphi = 0^\circ$ with red circles.



have one peak at about 20 meV. When the angle decreases ($\theta = 45^\circ, 30^\circ$, and 0°) this peak remains, but an additional peak appears at about 30 meV. In contrast to the sensitivity of the densities of states to the polar angle, the spectra at two azimuthal angles ($\varphi = 90^\circ$ and 0°) coincide.

For all crystal orientations, the calculated Lamb-Mössbauer factors are 0.82(2). In contrast to the pronounced anisotropy of the projected densities of states they do not depend on the crystal orientation. Although this is a surprise, it is not a contradiction, because the Lamb-Mössbauer factor is not very sensitive to the details of the density of phonon states. The constant value of the Lamb-Mössbauer factor along six non-equivalent crystallographic directions gives strong indication that the mean-square displacement of the iron atoms in the ferric borate crystal is mostly

isotropic with a value of $0.0042(5) \text{ \AA}^2$. In this concern we note that our results do not confirm the large anisotropy of the mean-square displacement reported earlier on the basis of crystal structure refinement.

The observed combination of the pronounced anisotropy of the density of phonon states and the isotropic mean-square displacement of the iron atoms give a striking example of the advantages of the nuclear inelastic absorption technique compared, for example, to Mössbauer spectroscopy, where the Lamb-Mössbauer factor is the only parameter to study the lattice dynamics. ■

REFERENCES

- [1] A.I. Chumakov, R. Rüffer, A.Q.R. Baron, H. Grünstedel, H.F. Grünstedel, V.G. Kohn, *Phys. Rev B* 56 (1997) 10758.
- [2] V.G. Kohn, A.I. Chumakov, R. Rüffer, *Phys. Rev. B* 58 (1998) 8437.



STROBOSCOPIC DIFFRACTION IMAGING OF HIGH-FREQUENCY SURFACE ACOUSTIC WAVES

E. ZOLOTUYABKO¹, D. SHILO¹, W. SAUER², E. PERNOT^{3,4} AND J. BARUCHEL³

¹ TECHNION, ISRAEL INSTITUTE OF TECHNOLOGY, HAIFA (ISRAEL)

² LMU MÜNCHEN, (GERMANY)

³ ESRF, EXPERIMENTS DIVISION

⁴ INPG, GRENOBLE (FRANCE)

Surface acoustic waves (SAWs) are widely used in communication systems. The visualization of the wavefronts is important because it gives clues about the defect-related dissipation of acoustic energy, which is detrimental for the device efficiency.

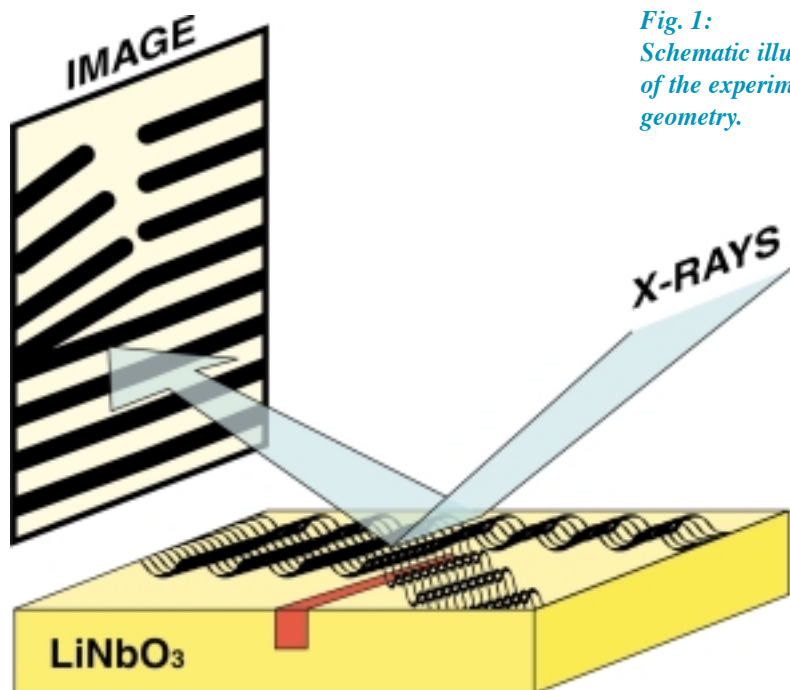


Fig. 1:
Schematic illustration of the experimental geometry.

X-ray diffraction imaging (x-ray topography) of the wavefronts has, in the past, been achieved for 30 MHz (wavelength $\sim 100 \mu\text{m}$) SAWs [1, 2]. The new possibilities provided by the ESRF allow to overcome the spatial resolution limitations encountered by the previous authors, and extend the visualization of SAW wavefronts to the frequency range presently used for the applications. The sample is a high-frequency ($\nu = 290\text{-}350 \text{ MHz}$, wavelength $\sim 10 \mu\text{m}$) LiNbO_3 -based SAW device, featuring a thin near-surface waveguide layer produced by the He ion implantation (Figure 1).

Traveling SAWs cause a long-range variation of elastic strain, which at any instant exhibits spatial periodicity over the whole crystal area. The modification of the x-ray intensity under SAW excitation is due to the corrugation of initially flat atomic planes. Stroboscopic diffraction imaging provides a "snapshot" of the SAW propagation, by accumulating images recorded at a given phase of the period. This was carried out by using an electrical signal associated with the pulsed x-ray beam from the storage ring

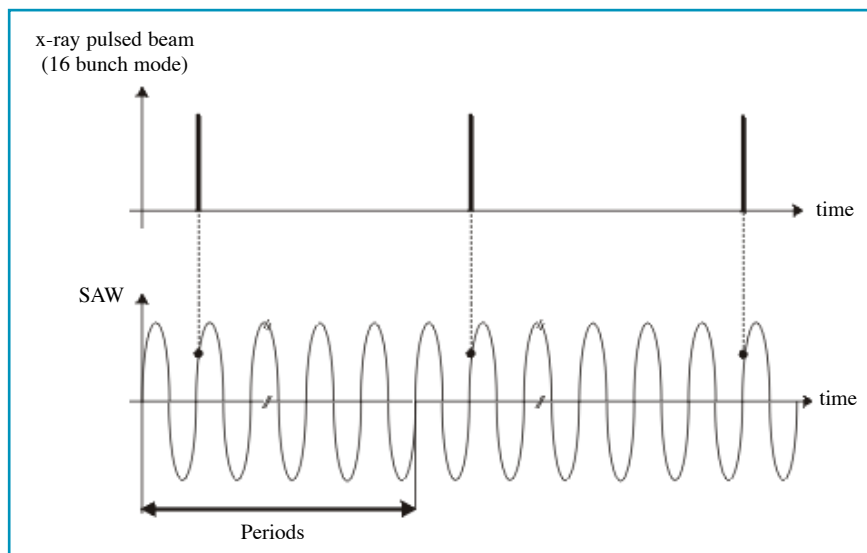
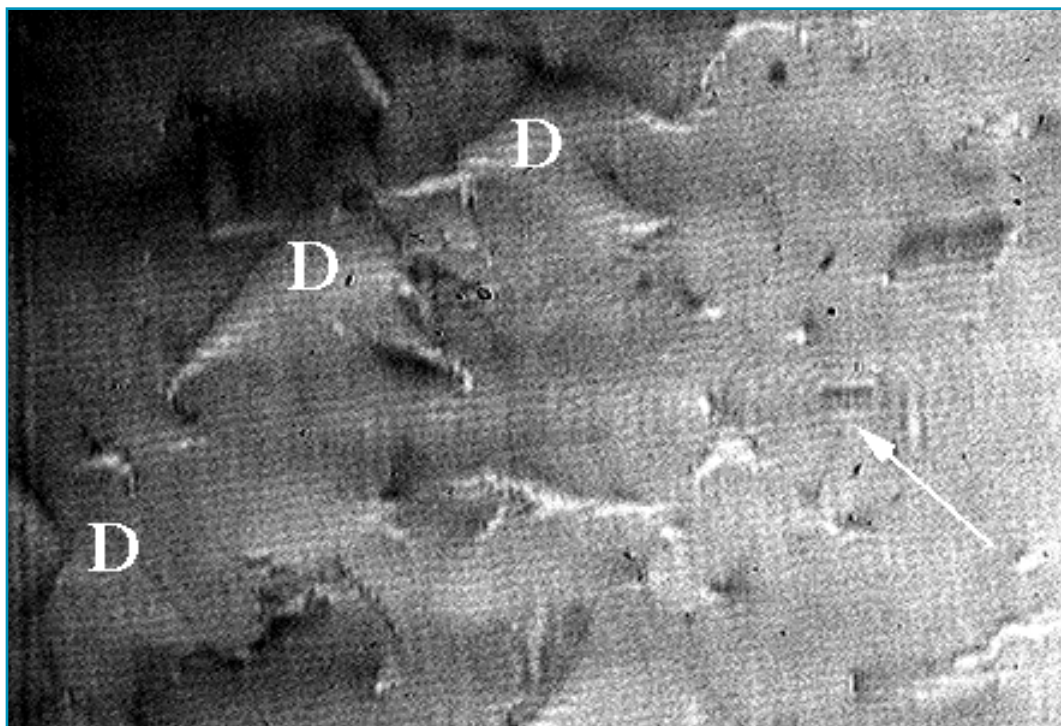


Fig. 2: Principle of stroboscopic diffraction imaging: the x-ray pulses always correspond to the same phase of the SAW at a given point of the crystal surface, allowing to sum up the diffracted beams up to required exposure time.



Fig. 3: Stroboscopic x-ray topograph of an as-implanted LiNbO₃ crystal (He ion energy - 320 keV, dose - $2 \cdot 10^{16} \text{ cm}^{-2}$) under SAW excitation. Crystal-film distance 23 cm. The acoustic ruler, introducing a 10- μm scale into the image, corresponds to the SAW wavefronts. Dislocations are indicated by the letters D. The location of the scattering center giving rise to secondary circular waves is indicated by an arrow.



operated in the 16-bunch mode, multiplied in frequency by an integer to drive the SAW device in a phase-locked mode, as schematically indicated on Figure 2.

X-ray topography was performed at the ID19 beamline, in the 16-bunch mode ($\nu_r = 5.68 \text{ MHz}$), *in situ*, under SAW excitation ($n = 51 \times \nu_r = 289.68 \text{ MHz}$ or $\nu = 62 \times \nu_r = 352.16 \text{ MHz}$). The images taken from such a modulated structure showed individual SAW wavefronts (alternating bright and dark lines, passing like a ruler through the image), as well as wavefront distortions, caused by basal screw dislocations D, as can be seen in Figure 3.

In addition, another scattering object, which we believe to be a He bubble, is visible in Figure 3 due to the secondary circular waves it produces. Secondary waves propagate away (at a distance of hundreds of micron) from the scattering center, like the waves that radiate from a stone plunged into water. A magnified picture of the circular elastic waves emanating from one of the bubbles is shown in Figure 4.

In fact ion implantation into single crystals is an important process in microelectronic and optoelectronic device technologies. It produces strain and defects within a thin layer buried at the ion stopping depth. Very small

defects, such as submicron bubbles, may affect the device characteristics even though they are invisible on standard x-ray topographs. It was found that a combination with short-wavelength SAWs results in an enhancement of the x-ray topographic contrast. When SAWs cross crystal regions containing extended defects, the individual wavefronts are distorted due to the scattering of acoustic power. Correspondingly, the acoustic ruler in the x-ray image becomes bent (see Figure 1), revealing defects which are not visible without the SAW. In the case of bubbles or cavities, which affect SAWs as strong density perturbations, secondary elastic waves arise, facilitating defect visualization.

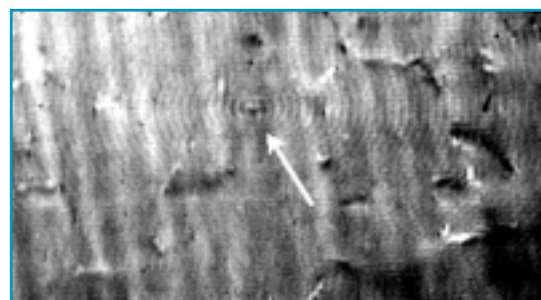


Fig. 4: X-ray topograph showing a picture of the secondary circular waves diverging from a He bubble (indicated by an arrow).

Analysis of all the collected images showed that the bubbles in our samples are 300-400 μm away from each other. The formation of a bubble thus appears to be a rare event, difficult to visualize except when benefiting from this "see-SAW" stroboscopic x-ray diffraction imaging technique [3]. ■

REFERENCES

- [1] R.W. Whatmore, P.A. Goddard, B.K. Tanner, G.F. Clark, *Nature* **299**, 44 (1982)
- [2] H. Cerva, W. Graeff, *Phys. Status Solidi A* **82**, 35 (1984)
- [3] E. Zolotoyabko, D. Shilo, W. Sauer, E. Pernot, J. Baruchel, *Appl. Phys. Lett.* **73**, 2278 (1998)



3D VISUALIZATION OF SNOW SAMPLES BY MICROTOMOGRAPHY AT LOW TEMPERATURE

J.-B. BRZOSKA¹, C. COLÉOU¹, B. LESAFFRE¹, S. BOREL², O. BRISSAUD³, W. LUDWIG⁴, E. BOLLER⁴ AND J. BARUCHEL⁴

1 MÉTÉO-FRANCE/CENTRE D'ÉTUDES DE LA NEIGE, GRENOBLE (FRANCE)

2 LCPC-LMSGC/CNRS, MARNE-LA-VALLÉE (FRANCE)

3 LGGE/CNRS, GRENOBLE (FRANCE)

4 ESRF, EXPERIMENTS DIVISION

Snow on the ground is a mixture of ice particles, air and occasionally liquid water and it can take different aspects. In most cases, recent snow is a very loose powder, which can transform into hard, crusted or pasty material. This means that each snowfall undergoes metamorphism [1, 2] according to weather conditions and exposure, leading to a layered snowpack.

The growth of ice particles is caused by vapor diffusion in dry snow and melt-freeze exchanges in wet snow. Normally, dry snow covers are warmer on the bottom than on the top. The value of the temperature gradient determines whether rounded (small gradient) or faceted crystals (large gradient) will grow [3].

Metamorphism has huge consequences: the physical and mechanical properties of the different snow layers can change dramatically, commonly over several orders of magnitude. In some cases the snow crystals are able to stick on vertical rocks, whereas in other cases just one skier can release a slab avalanche of several thousand tons. The shape and arrangement of the grains and the quality of the ice bonds will govern the snow properties.

The important parameters describing the state of a snow layer are the specific area, the grain connections and the local grain curvature. They cannot be directly derived from classical two-dimensional (2D) observations. For the first time, tomographic methods provide data on the three-dimensional (3D) microstructure of snow that is both statistically significant because it represents a large number of grains, and at a high resolution compared to the grain scale.

EXPERIMENTAL TECHNIQUE

Microtomography is an established technique for the 3D visualization of quite diverse objects, with spatial resolution better than 20 μm . Many 2D images are recorded at angular positions of the object around an axis (vertical in our case) spanning 180°. "Tomographic" reconstruction provides, from the 2D images, and

via appropriate algorithms and programs, the 3D information from which cuts, projections, or perspective renditions of the object can then be obtained at will. The number of 2D images necessary is approximately equal to the number of pixel columns used by the image on the detector. At the ID19 imaging and diffraction beamline at the ESRF this number is usually between 600 and 900. The time needed for recording the 2D images is of the order of an hour, and a few hours are needed for the computer reconstruction of the 3D image.

In the case of snow, a cryostat specially designed for image recording, i.e. displaying a homogeneous behavior over the whole angular range, was used. Its main features are a regulated nitrogen (-60°C) gas flow to cool the sample, which sits in a cylindrical enclosure with double plexiglas walls, 0.5 mm thick and polished. **Figure 1** shows the cryostat, the rotation stage, and the Frelon CCD camera [4] used to record the images.

SAMPLE PREPARATION AND RESULTS

3D views of three different snow samples are shown in **Figure 2**. For samples (a) and (b), fresh snow, collected on the field, was allowed to evolve in a cold laboratory. The sample (a) was obtained by immersion in water at 0°C : it consists of well-rounded grains; the mean convex radius of curvature computed from 2D images of grain outlines [5] was $\langle r \rangle = 0.25$ mm. The sample (b) was transformed under the action of a large temperature gradient (of the order of $1^\circ\text{C}/\text{cm}$) applied during eight days; due to experimental problems, this temperature gradient was not maintained the following three days. It exhibits faceted crystals: $\langle r \rangle = 0.17$ mm, estimated grain size: 0.4 mm. The third sample (c) is a melt-freeze crust, partially faceted under a natural temperature

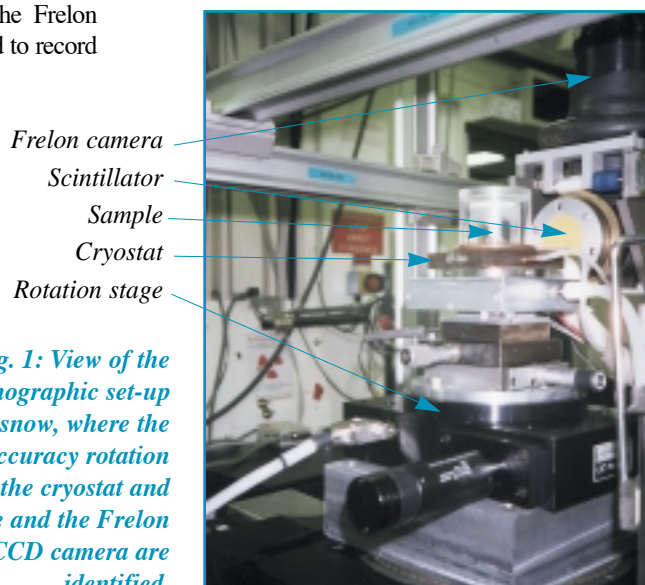


Fig. 1: View of the microtomographic set-up used for snow, where the high accuracy rotation stage, the cryostat and sample and the Frelon CCD camera are identified.



Fig. 2: 3D views of snow reconstructed from 1000 tomographic images. Image size is 600^3 voxels, voxel size is $10\ \mu\text{m}$, exposure time 1s/view.

(a): wet snow, energy 12 keV.

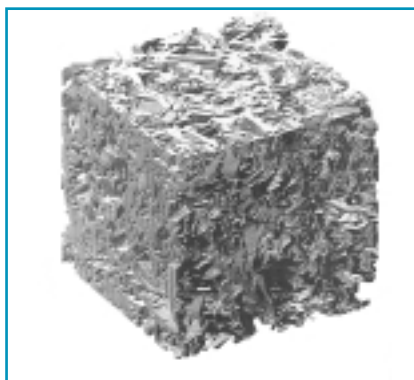


Fig. 2(b): faceted crystals, energy 10 keV.



Fig. 2(c): melt-freeze crust, energy 10 keV.

gradient: $\langle r \rangle = 0.25\ \text{mm}$. It was collected on the field at Col de Porte (1340 m, Chartreuse mountain, France).

Those three samples were then prepared in the cold laboratory. To prevent sublimation and grain damage during sample machining and handling, the snow structure was strengthened by using diethyl-orthophthalate [6] (phthalate for short, m.p. -5°C). Before any handling, liquid phthalate was poured at -5°C on snow, and allowed to freeze at -20°C . Frozen lumps of $\approx 100\ \text{cm}^3$ were then extracted and machined at -20°C , in the cold laboratory, into cylinders 10 mm high, with diameter 10 mm. Phthalate was then removed by rinsing in isoctane at -2°C . Isoctane was then drained from the sample (10 s on blotting paper), finally quickly evaporated under vacuum (30 s). The sample was put in a gas-tight cylindrical sample holder and stored in a cool box with CO_2 dry ice until the start of the experiments, in order to prevent sublimation.

The quality of the reconstructed images shows that the samples neither

moved nor evolved during tomography.

DISCUSSION

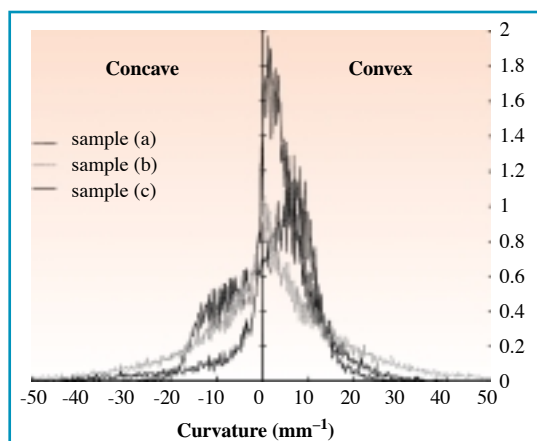
Curvature has long been recognized as a central parameter in snow microphysics. Its importance derives from the fact that the pore size distribution of snow clusters is in the capillary range (0.1 - 1 mm). The structure of snow evolves with temperature and humidity fields, with a specially strong effect of the presence of liquid water when the temperature reaches 0°C . Except at the high sublimation rates leading to faceted shapes, these structure modifications are governed by local curvature.

Until recently, only the 2D local curvature of grains could be used. This gave valuable information on grain types for modeling snow metamorphism but could not, for instance, account correctly for water percolation. The availability of 3D information directly from tomography makes it possible to use the full curvature. We have developed a

code for curvature computation from the 3D images, and we checked it on a set of microtome serial cuts of refrozen wet snow [7]. Applying this code to the data files obtained for the above three samples (a, b, c) produced the curvature histograms shown in Figure 3. Samples a, b, c, obtained through three different physical processes as described above, lead to three quite different curvature «signatures». For instance, the histogram of refrozen snow (sample a) shows two modes. One of them, being positive, is characteristic of grain size. The other mode points out negative curvatures and should correspond to interconnected liquid water menisci (concave).

Tomography high resolution images will allow further investigation of other features of snow microstructure such as specific area, relevant for metamorphism dynamics, or ice bond geometry, relevant for mechanical and thermal properties. ■

Fig. 3: Histogram of 3D local curvature of grain surface computed from a 128^3 voxels subsample of each image. This curvature is defined at any point as $1/R_1 + 1/R_2$ where R_1 and R_2 are radii of curvature in any pair of orthogonal planes containing the normal vector.



REFERENCES

- [1] S. C. Colbeck, *Journal of Geophysical Research*, 1983, 88, pp. 5475-5482
- [2] E. Brun, *Ann. Glaciol.*, 1989, 13, pp 22-26
- [3] S. C. Colbeck, E. Akitaya, R. Armstrong, H. Gubler, J. Lafeuille, K. Lied, D. McClung, E. Morris, 1990, Wallingford, Oxfordshire, International Association of Hydrological Sciences
- [4] J.C. Labiche, J. Segura Puchades, D. Van Brussel and J.P. Moy, *ESRF Newsletter* p. 41, March 1996
- [5] B. Lesaffre, E. Pougatch and E. Martin. 1998. *Ann. Glaciol.* 1998, 26, pp 112-118
- [6] W. Good, *International Association of Hydrological Sciences*, 1987, Nr 162, pp 35-48
- [7] J.B. Brzoska, B. Lesaffre, C. Coléou, K. Xu, R. A. Pieritz, submitted to *Eur. J. Appl. Phys.*

Events

Users' Meeting

11 February 1999

A record number of participants was registered for this ninth ESRF Users' Meeting. For the first time, it took place in February and was caught in exceptionally heavy snowstorms!
(See page 3)



Young Scientist Award goes to Peter Cloetens

(See page 3)



Appointment of a new Director General

Yves Petroff, the present ESRF Director General, will leave his function at the end of the year 2000.

As the first step towards his succession, the eight delegations to the ESRF Council are invited to nominate candidates.

(See page 2)